# SHEAR STRENGTH OF CANADIAN SOFTWOOD STRUCTURAL LUMBER

by

Hon Wing Yee

B.A.Sc. (Civil Engineering) University of British Columbia, 1991

A THESIS SUBMITTED IN PARTIAL FULFILLMENT OF

THE REQUIREMENTS FOR THE DEGREE OF

MASTER OF APPLIED SCIENCE

in

THE FACULTY OF GRADUATE STUDIES

Department of Wood Science

We accept this thesis as conforming

to the required standard

The University of British Columbia

December 1995

In presenting this thesis in partial fulfilment of the requirements for an advanced degree at the University of British Columbia, I agree that the Library shall make it freely available for reference and study. I further agree that permission for extensive copying of this thesis for scholarly purposes may be granted by the head of my department or by his or her representatives. It is understood that copying or publication of this thesis for financial gain shall not be allowed without my written permission.

Department of Wood Science

The University of British Columbia
Vancouver, Canada

Date DECEMBER 22, 1995



DE-6 (2/88)

## ABSTRACT

An experimental study has been conducted to evaluate the longitudinal shear strength of Canadian softwood structural lumber using a two span five point bending test procedure. Nominal 38mm x 185mm Douglas-Fir, nominal 38mm x 185mm and nominal 38mm x 285mm Hem-Fir and Spruce-Pine-Fir boards have been considered. Flat-wise and edge-wise modulus of elasticity tests have been conducted for each specimens prior to the destructive shear tests.

A two span five point bending test procedure has been chosen because of its ability to produce a relatively high percentage of longitudinal shear failures. Approximately 40% of the failures can be attributed to shear failures in the nominal 38 mm x 185 mm and 30% in the nominal 38 mm x 285 mm specimens. Two test configurations have been considered: test span to specimen depth ratios of 6:1 and 5:1.

American Society for Testing and Materials (ASTM) shear block tests have also been conducted to evaluate the shear strength of small clear specimens. Based on the ASTM shear block test and the edge-wise modulus of elasticity results, a linear elastic finite element analysis coupled with Weibull weakest link theory has been used to predict the shear failure loads at different levels of failure probability. Good agreement between predicted and measured failure loads at different probability of failure levels for the different sizes and spans of each species have been observed.

Predictions from the finite element and size effect analysis procedures have been compared to an empirical approach for predicting longitudinal shear resistance in sawn lumber and glued laminated beams proposed by the US Forest Products Laboratory. The US proposed design equation tends to overestimate the longitudinal shear resistance of the full size beam results obtained from this study.

In lower grades of dimension lumber, shear failures do not govern because the bending to shear strength ratio is usually significantly lower as compared to the Select Structural grade material. Therefore in the lower quality dimension lumber, bending failure mode would most likely dominate.

TABLE OF CONTENTS

## LIST OF TABLES

## LIST OF FIGURES

## LIST OF SYMBOLS

$\tau$ = full size beam shear strength (psi)

$A$ = Shear Area= area of beam subjected to shear forces.

$C_f$ = stress concentration factor to adjust the ASTM shear block to the true shear stress distribution. It is assumed to be 2 (Soltis and Rammer 1994)

$\tau_{ASTM}$ = ASTM D143 published shear block values

$P_{fA}$ = probability of failure in lumber free from end splits and cracks, failure mode (case A)

$P_{fB}$ = probability of failure in crack propagation mode (case B)

$a_o$ = is the critical crack length which governs the type of shear failure mode
if the crack length, a, is $< a_o$, failure mode is case A
if the crack length, a, is $> a_o$, failure mode is case B

a = is a random variable representing the crack length found within a population of lumber

$\gamma$ = the ratio of nominal dead to nominal live load

V = total volume of the beam

$\varsigma$ = is the geometric factor depending on the loading condition

$d$ = is a random variable representing total applied dead load divided by nominal dead load

q = is a random variable representing total applied live load divided by nominal live load

$\tau^*$ = shear strength of a unit volume under uniform shear

$\lambda$ = was taken as 1.95 for softwood based on ASTM shear blocks for air-dry Douglas fir (Kennedy 1965), which was assumed to be also species independent

$\tau_{ASTM}$ = ASTM shear block shear strength

$P_{failure}$ = probability of failure

$\phi$ = Performance or Resistance factor = 0.9

$F_v$ = $f_v$ ( $K_D$ $K_H$ $K_{sv}$ $K_T$ )

$A$ = Area of cross section (b x d), $mm^2$

$K_{ZV}$ = size factor in shear ( CSA-086.1 Table 5.4.5)

$K_N$ = notch factor

$f_v$ = specified strength in shear ( CSA-0.86.1 Table 5.3.1A to 5.3.1D ) MPa

$K_D$ = load duration factor

$K_H$ = system factor

$K_{sv}$ = service condition factor for shear

$K_T$ = treatment factor

$\tau_{0.5}^*$ = the median uniform shear stresses over the unit volume.

$\sigma(x,y,z)_{beam\ 0.5}$ = the shear stress field associated with the median shear failure load over the beam volume .

$\sigma(x,y,z)_{input}$ = the shear stress field associated with the input load $P_{input}$ for the program FEMPC.

$\sigma(x,y,z)_{beam}$ = the shear stress field associated with the load $P_{beam}$ of the beam
$\tau_{ASTM}$ = Shear stresses for the ASTM shear block.
$CV$ = coefficient of variation of shear strength.
b = beam width
d = beam depth
$\Delta$ = deflection at center
$E_{flat}$ = flat-wise modulus of elasticity (MOE)
$I_y$ = moment of inertia. For a rectangular beam section on flat
h = thickness of the beam.
$E_{edge}$ = edge-wise Modulus of Elasticity (MOE)
P = applied load
$\Delta_c$ = displacement measured by the yoke's LVDT at point C relative to line AB.
L = span between the supports
$I_x$ = moment of inertia for the rectangular beam about the strong axis.
$WT_{od}$ = oven dry weight of the blocks
$V_{od}$ = oven dry volume of the blocks
$\rho_w$ = density of water = 0.001 g/mm$^3$
$E_{perd}$ = modulus of elasticity perpendicular to grain in psi
$E_{edge}$ = edge-wise modulus of elasticity in psi
G = shear modulus in psi

## ACKNOWLEDGMENT

I would like to thank Dr. Frank Lam for his tremendous guidance and input throughout this research. In addition, I would also like to express my sincere thanks to Drs. J.D. Barrett and H. Prion who have made this research project possible.

Other thanks goes to the supportive technical staff members of the Department of Wood Science, Bob Myronuk, and Paul Symons of the Department of Civil Engineering.

Finally, COFI, Forestry of Canada, NLGA, NSERC and Weyerhaeuser are thanked for their donations of the testing materials and financial support.

# 1. INTRODUCTION

## 1.1 LONGITUDINAL SHEAR STRENGTH OF DIMENSION LUMBER

The longitudinal shear strength of sawn lumber is important because it governs the design of beams with small span-to-depth ratios. Shear design provisions for sawn lumber members in working stress design codes are believed to be unnecessarily conservative for many common applications. Under realistic loading and support conditions, tests results have shown that it is very difficult to obtain pure shear failures in members, especially when the members do not have end splits. The conservative design provisions lead to shear controlled design in cases where experience suggests that shear failure is not a probable failure mode.

The Canadian Code for Engineering Design in Wood has adopted new design provisions for shear design of lumber members which recognize a significant size effect in member shear capacity. The design procedure provides for much larger characteristic strength properties for smaller sections, reflecting the size effects in wood material strength and the size effect in the strength of notched members.

Two distinct failure modes can be observed during shear strength tests of lumber. These failure modes are controlled by: 1) the shear strength of the material when end split or other similar defects are not present and 2) the crack length and mode II fracture toughness ($K_{IIC}$) in members where parallel to grain end split defects exist (Foschi and Barrett 1976). To account for these two modes of failure, development of allowable shear stresses for lumber in North America

traditionally followed provisions of the American Society for Testing and Materials (ASTM) standard D245 (ASTM, 1994b). Small clear straight-grain shear block specimens are first tested in shear. The shear block test results are modified by a reduction factor of 4.1 to account for safety and load duration (1.82), and stress concentrations (2.25) due to strength reducing characteristics in commercial full size material. The effect of end cracks, checks or splits is then considered by the introduction of another factor, S:

$$S = 1 - \frac{a}{3H} \qquad [1]$$

where S is the strength ratio which is multiplied to the clear beam shear strength value to account for the effect of end cracks, checks or splits, and a is the crack length and H is the member depth. The use of ASTM shear block test results, to first determine the shear capacity of small clear specimens and then adjust for natural defects in lumber, is somewhat inconsistent with the in-grade philosophy of testing full size members, which has been adopted worldwide for the development of characteristic strength properties of structural lumber. The major difficulty associated with testing for longitudinal shear strength of full size lumber using a typical test setup is that the members usually fail in other modes such as bending or compression perpendicular to grain, especially in members which do not contain end-splits.

Shear design provisions in the Canadian Code for Engineering Design in Wood (Foschi, Folz, and Yao 1989) are based on the two-parameter weakest link theory for predicting member resistance for the clear-beam mode. Weakest link shear capacity models have been developed for Douglas-Fir using data from ASTM shear block tests, small beam tests, torsion tests and glued

laminated beam results (Foschi and Barrett, 1975). ASTM shear block results were used to generate weakest link size effect models for untested species (Foschi, Folz, and Yao, 1989). The predicted shear resistance models have not been verified with tests of dimension lumber size members.

A two span five point bending test procedure, originally developed for the evaluation of the shear strength of composite materials, has been proposed for testing of the shear strength properties of full size lumber. Experimental programs in the US Forest Products Laboratory and the Commonwealth Scientific and Industrial Research Organization (CSIRO) in Australia have successfully used this two span five point bending test setup to evaluate the shear strength of glued-laminated beams and full-size commercial lumber (Leicester and Breitinger 1992, Breitinger *et al.* 1994, Soltis and Rammer 1994). In the US Forest Product Laboratory and CSIRO test programs, span to depth ratios of 5:1 and 6:1 were used respectively. The span was defined as the distance between the center of the end reaction to the center to the middle support.

Past studies, based on the Weibull Weakest Link concept (Weibull, 1939), demonstrated that member shear strength capacities depend strongly on the test configuration, member size, and stressed volume (Foschi and Barrett 1976, 1977a, 1977b, Liu 1980 and 1981). Clear understanding of the measured test results in relation to the different test configurations is necessary before new test procedures can be adapted for standards and conversion of test data into design properties.

In this project, an experimental study was conducted to evaluate the longitudinal shear strength of three species groups and two sizes of Canadian softwood dimension lumber using a two span five point bending test set up. Two test configurations were considered: test span to specimen depth ratios of 6:1 (6D case) and 5:1 (5D case). The test span is the distance between the center of the end reaction to the center to the middle support.

A procedure based on finite element (FE) analysis coupled with Weibull weakest link theory was used to predict shear failure loads at different shear failure probability levels of the lumber from ASTM shear block test results and to establish the relationships between the full size specimens test results from the two test configurations.

## 1.2 OBJECTIVE OF THIS STUDY

The purpose of this study was to develop an experimental database on material properties required for reliability studies of bending members in shear to support a proposal for international standardization of improved shear design provisions for structural lumber.

# 2. BACKGROUND INFORMATION

## 2.1 HISTORY OF SHEAR STUDIES

The subject of establishing parallel-to-grain allowable shear stresses for lumber has long been studied. The earliest documented reports of tests for large members date back to 1906 by Hatt ( Ethington *et al.* 1979). Although he had conducted tests with small specimens taken from failed pieces, a standard shear test did not exist at that time. The US Forest Products Laboratory began a research program in 1910 to evaluate the mechanical properties of small, clear, straight-grained specimens by species. Bulletin No. 108 (1912) contains a summary of data up to that time. This publication provided data for calculating both shear stresses in structural beams which failed in shear and those which failed in shear followed by other types of failures.

Keenan (1974) suggested that the shear strength of Douglas-Fir glued-laminated beams depends on the shear area. The shear area defined by Keenan is the shear span multiplied by the beam's width. The shear span is the distance between supports. This shear area can be easily defined for concentrated loading conditions, but is undefined for uniformly distributed loads.

Barrett and Foschi (1976, 1977) applied Weibull's theory of brittle fracture to determine the strength of Douglas-Fir wood in longitudinal shear. Given a certain survival probability, they have derived the ultimate stresses for beams under different loading conditions. The theory explains the discrepancy between the shear resistance of the ASTM shear blocks and a full size

beam. They related the shear strength of a unit volume under uniform shear stresses (based on the ASTM shear blocks results) to the shear stress volume defined by Weibull's weakest link theory of the full size beam.

Longworth (1977) used a four point bending test with small length-to-depth ratios on 150 glued-laminated Douglas-Fir beams. He concluded that the ASTM shear block strength badly represents the shear resistance of full size beams. Using the definition of shear area by Keenan et. al. (1974), Longworth showed that shear strength decreases for larger shear area.

Recently, Rammer and Soltis (1994) suggested that the shear strength of full size beams is a function of shear area which relates to the ASTM shear block by the following equation;

$$\tau = \frac{1.3 C_f \tau_{ASTM}}{A^{\frac{1}{5}}} \qquad [2]$$

where,

$\tau$ = full size beam shear strength (psi)
$A$ = Shear Area[1] = area of beam subjected to shear forces.
$C_f$ = stress concentration factor to adjust the ASTM shear block to the true shear stress distribution. It is assumed to be 2 (Soltis and Rammer 1994)
$\tau_{ASTM}$ = ASTM D143 published shear block values

The shear area defined by Soltis and Rammer (1994) is different from that defined by Keenan et. al. which states the shear area as the span between the load and the support under only positive shear, multiplied by the width. No reason was indicated as to the different consequences for selecting either positive or negative shear. Soltis and Rammer define the shear area as the span

[1] Shear Area defined by Soltis and Rammer as the length of the beam subject to positive and negative shear multiple by the width of the beam. (inch$^2$.)

between the loads and supports under both positive and negative shear, multiplied by the width of the member.

Soltis and Rammer (1994) conducted a five point full size beam shear test. Figure 1 shows the full size shear test setup for nominal 38mm x 204mm boards. A span of five times the depth of the beam was used between the supports. The loading position was at mid-span between the center and edge supports. The corresponding sizes of the loading plates and supports are given in Figure 1. The load was monotonic with a rate of loading that conforms to the ASTM D 198 (1994b) standard which specifies that the beam should fail between 6 to 20 minutes. Problems were reported related to the beams rotating out of the plane of loading. ASTM shear blocks were obtained from the members that failed in shear near the region of failure but away from any visible damage. These blocks were later used in the computation of equation 2 .

Their five point shear test was able to produce a 62% success rate (99 out of 160 Douglas-Fir solid sawn lumber of different sizes) in shear failures. Most shear failures were reported to be between the middle support and the loading point which rarely propagated past the loading point. Their coefficient of variation for the beam shear strength was under 20% with an average of 14.2%. The coefficient of variation for the ASTM shear blocks was between 12.7 % to 18.8 % for the dry specimens.

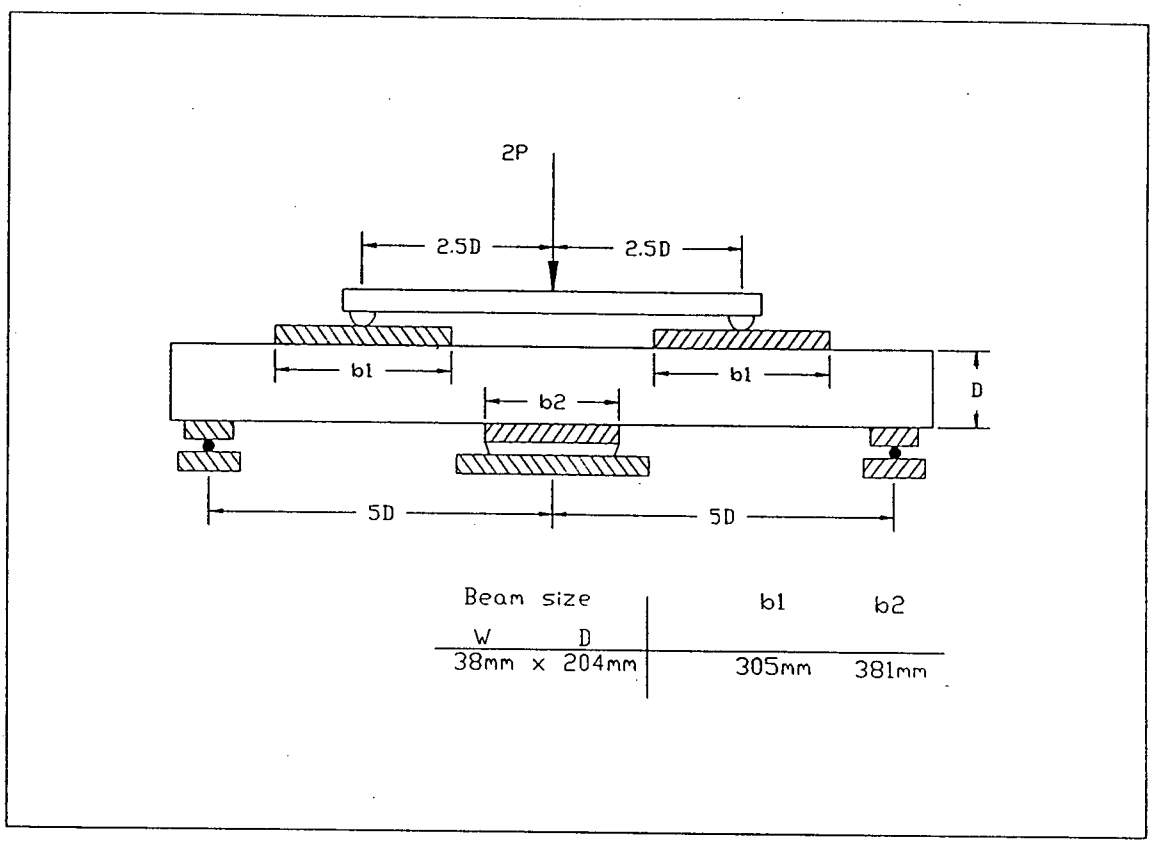


Figure 1. 5 point test setup used by Soltis and Rammer

## 2.2 THE BASIS FOR THE CURRENT SHEAR DESIGN PROVISION

Shear design provisions for working stress design codes are considered to be overly conservative for many common applications. The establishment of allowable shear stresses for lumber used in working stress design codes in the US followed the provisions of ASTM D 245.

The fifth percentile shear strength from small clear shear block test data for softwood are modified by a factor of 4.1 to provide a basic allowable shear stress for beams free from shakes, checks or splits. Design for shear resistance is receiving considerable attention as the occurrence of shear controlled design seems to govern in situations where experience suggests that shear controlled failures are uncommon.

The Canadian Code for Engineering Design in Wood (CAN3/CSA-086.1-M89) contains provisions for shear design of solid sawn lumber based on reliability principles. The member shear resistances are established with recognition of two potential failure modes analogous to the ASTM procedures. The shear capacity of beams free from shakes, checks, or splits is determined by the inherent shear strength of the clear material. The presence of shakes, checks, or splits reduces the " the clear-member" mode to a "beam-defect" mode. Several beam-defect failure modes are possible, associated with shear failure due to end-splits, surface checks or shakes. The evaluation of member reliability requires knowledge of the shear resistance for the clear-member and each of the beam-defect modes and data on probability of occurrence of each failure mode.

The clear-wood failure mode has been studied using the two-parameter Weibull weakest link concept to provide a basis for explaining the different shear strengths observed between small clear ASTM shear blocks and full size beam members, which relates the shear strength to member size, shape and loading conditions (Foschi and Barrett, 1976). This study has confirmed that the shear strength varies with the type, size and shape of shear test specimens.

Linear elastic fracture mechanics concepts were also used to study the shear capacity of beams containing parallel-to-grain cracks analogous to the end-splits, checks and shakes observed in structural wood members. A linear elastic fracture mechanics analysis allows the capacity of bending members with parallel-to-grain defects to be predicted when the material fracture toughness is known. Shear resistance of beams must be known for each shear failure mode (end-split mode, check and shakes mode). Reliability in shear can be calculated when the type and extend of each defect and the probability of occurrence of each failure mode is known.

A reliability based approach has been adopted in Canada to relate ASTM shear block strengths with full size members by Foschi et al. (1989). To evaluate the probability of longitudinal shear failure, $P_f$, in a population of full size lumber, two distinct failure modes must be considered as follows:

$$P_f = P_{fA}\,[Probability(0 \le a \le a_o)] + P_{fB}\,[Probability(a \ge a_o)] \qquad [3]$$

where,

$P_{fA}$ = probability of failure in lumber free from end splits and cracks, failure mode (case A)

$P_{fB}$ = probability of failure in crack propagation mode (case B)

$a_o$ = is the critical crack length which governs the type of shear failure mode
if the crack length, a, is $< a_o$, failure mode is case A
if the crack length, a, is $> a_o$, failure mode is case B

a = is a random variable representing the crack length found within a population of lumber

Considering first only lumber free from end splits and cracks (case A), the reliability based limit state design equation in the Canadian Design Code, CAN3-086.1-M89, states the following:

$$1.25E(D_n) + 1.50E(Q_n) = \Phi R_C$$

[4]

where, $E(D_n)$ and $E(Q_n)$ are, respectively, the nominal dead and live load effects and $\phi$ is a performance factor applied to the characteristic or specified shear strength $R_c$.

During the code development process, in order to evaluate $\phi$ and $R_c$ for equation 4, a performance function, $G_1$, associated with lumber free from end splits and cracks (case A) was evaluated. An example of a performance function for a beam under uniformly distributed load is as follows:

$$G_1 = \frac{\zeta \tau^*}{V^{\frac{1}{k}}} - \frac{2 \Phi R_c}{(1.25\gamma + 1.5)}(\gamma d + q)$$

[5]

where

$\gamma$ = the ratio of nominal dead to nominal live load
V = total volume of the beam
$\varsigma$ = is the geometric factor depending on the loading condition
$d$ = is a random variable representing total applied dead load divided by nominal dead load
q = is a random variable representing total applied live load divided by nominal live load
$\tau^*$ = shear strength of a unit volume under uniform shear

Since shear test data were not available for dimension lumber, $\tau^*$ was calculated using the following expression:

$$\tau^* = m[-\ln(1 - P_{failure})]^{\frac{1}{k}}$$

[6]

where

$k$ = was taken as 5.53 for softwood based on glued-laminated lumber test results (Foschi and Barrett 1975), which was assumed to be species independent.
$P_{failure}$ = is the probability level of failure.

The scale parameter, m, is given by:

$$m = \lambda \tau_{ASTM} \qquad [7]$$

where

$\lambda$ = was taken as 1.95 for softwood based on ASTM shear blocks for air-dry Douglas fir (Kennedy 1965), which was assumed to be also species independent

$\tau_{ASTM}$ = ASTM shear block shear strength at the probability level of failure, $P_{failure}$.

The characteristic or specified shear strength, $R_c$ was determined from the mean ASTM shear block strength for dimension lumber, $\tau_{clear}$, of clear and green material adjusted to 5-th percentile level and dry conditions as:

$$R_C = \tau_{clear}(1 - 1.645cv)x1.08x2.25^{-1} \qquad [8]$$

where

$cv$ = coefficient of variation of the green strength

1.08 = is the adjustment for seasoning

$2.25^{-1}$ = is the traditional ASTM conversion factor from shear block to beam strength

The second mode of failure (case B) of equation 3, which involves a fracture toughness parameter ($K_{IIc}$), (Foschi, Folz, Yao 1989) was not considered in this study.

Achieving shear failure in small and short split-free lumber specimens has proven to be a major obstacle limiting improvement in shear design of split-free members. These small and short split-free lumber specimens tends to fail in compression perpendicular to grain rather then shear under the traditional bending test. Recently (Soltis, 1994 and Leicester, 1994) reported success in

achieving a high proportion of shear failures in sawn lumber beams using a two-span continuous beam test specimen. The two-span beam specimens exhibited several failure modes such as shear parallel-to-grain, bending (tension parallel to grain), and compression perpendicular to grain. With a satisfactory test method, the material property database necessary for reliability studies could be extended to a wider range of structurally important species.

Reliability studies conducted to date have assumed that the clear-beam and defect-beam failure modes are independent. This is a conservative assumption and additional experimental effort should be directed at establishing the relationship between shear strength of clear-beams and the fracture parameters associated with the crack propagation failure modes.

## 2.3 WORKING STRESS DESIGN (WSD) AND LIMIT STATES DESIGN (LSD)

In the Working Stress Design approach, the allowable shear stress is a fraction of the shear stress corresponding to failure. The design equation has the following form:

$$\textit{Applied Shear Stresses} \leq \textit{Allowable Shear Stresses} \qquad [9]$$

where allowable shear stress is the material strength ÷ safety factors and the applied shear stress is derived from a nominal load condition based on the probability of exceeding a certain limit within a certain time.

In accordance with current ASTM D245, the clear wood shear strength values obtained by ASTM D2555 (1994) are reduced by a factor of 4.1 for softwoods and 4.5 for hardwoods. This factor of 4.1 accounts for stress concentrations (2.25), and duration of load (1.82). The working stress design method is still being used in the US.

The more modern Limit State Design approach applies load factors to the nominal applied shear load and a resistance factor to the tested shear resistance of the member. This method has been adopted by the Canadian Design Code and more recently the European codes. The design equations and related factors are determined using a probabilistic approach to meet an overall level of safety, represented by the so-called safety index (Foschi, Folz, Yao 1989). Load and resistance factors are calibrated to meet this target. The design equation has the following form:

$$\textit{Factored shear resistance of structure} \geq \textit{Factored shear load effect} \qquad [10]$$

In accordance with CAN/CSA-086.1-M89, the factored shear resistance, $V_r$ of sawn lumber is

$$Vr = \phi F_v \frac{2}{3} A K_{ZV} K_N \qquad [11]$$

Where,

$\phi$ = Performance or Resistance factor = 0.9
$F_v$ = $f_v$ ( $K_D$ $K_H$ $K_{sv}$ $K_T$ )
$A$ = Area of cross section (b x d), $mm^2$
$K_{ZV}$ = size factor in shear ( CSA-086.1 Table 5.4.5)
$K_N$ = notch factor

$f_v$ = specified strength in shear [2]
( CSA-0.86.1 Table 5.3.1A to 5.3.1D ) MPa
$K_D$ = load duration factor
$K_H$ = system factor
$K_{sv}$ = service condition factor for shear
$K_T$ = treatment factor

Figure 2 compares the two design methods. The Limit State Design approach applies factors to the design load to account for various loading conditions. This approach yields a consistent safety margin for all structures regardless of on the loading conditions. In the Working Stress Design method, however, no differentiation is made between the different loading conditions or the structure type, which results in an inconsistent safety margin.

[2] $f_v$ depends on the species , grade, and usage. It ranges from 0.7 to 1.9 for species studied in this paper. ( Douglas-Fir, Hem-Fir, Spruce-Pine-Fir)

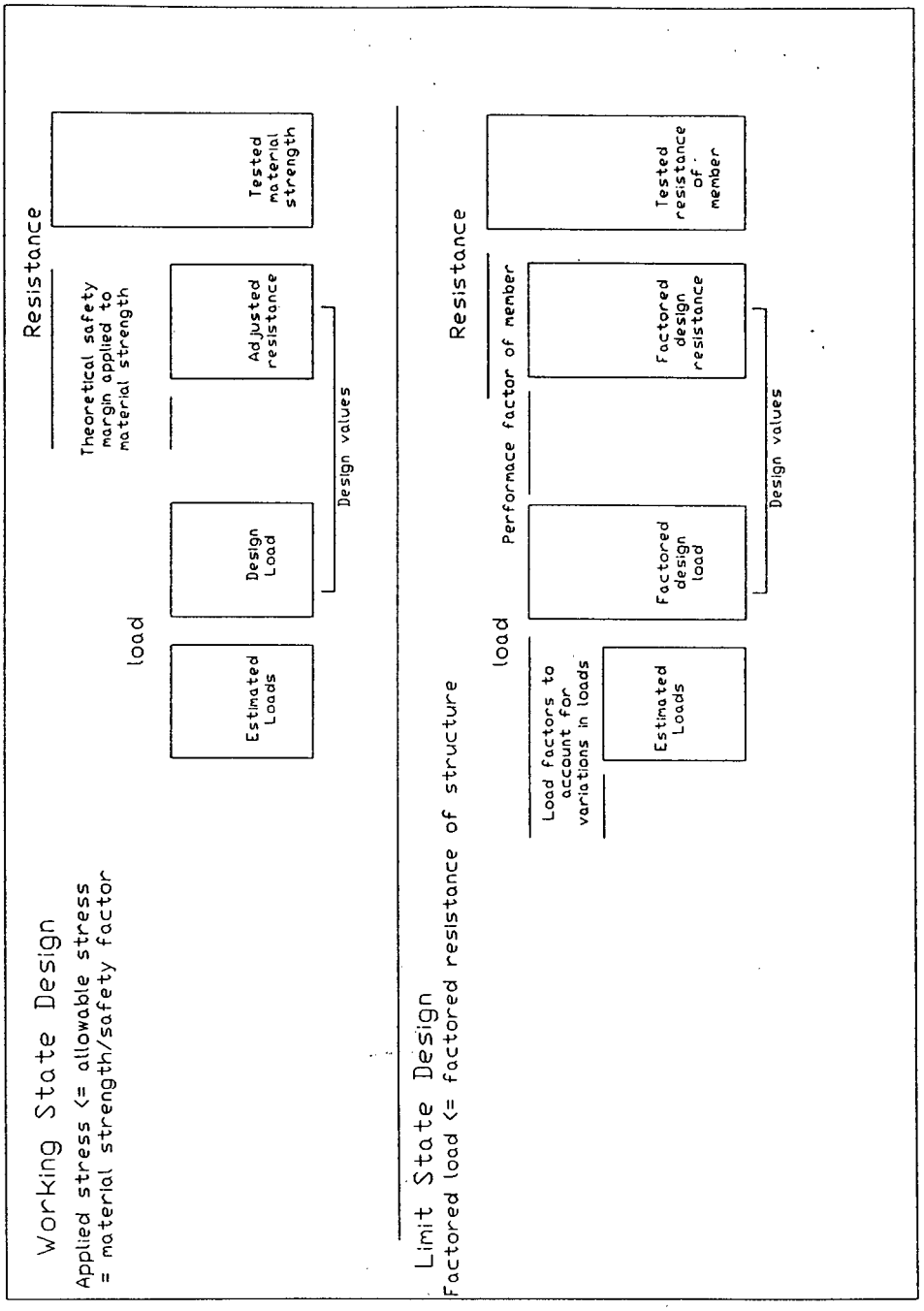


Figure 2. Comparison of Working State Design and Limit State Design methods.

# 3. THEORY AND ANALYSIS MODEL

## 3.1 WEIBULL WEAKEST LINK THEORY

The Weibull weakest link theory can be used to explain the effects of size and stress distribution in some materials. This approach is based on two major assumptions: Firstly, the member is expected to behave like a perfectly brittle material such as glass or steel at very low temperatures. For such perfectly brittle material, total failure occurs when fracture occurs at the weakest point. Secondly, the member is assumed to be made up of individual elements with random but statistically independent strengths. The weakest link theory states that the strength of the member is determined by the minimum strength value among all the elements.

Consider the shear strength of a unit volume of material with dimension 1mm x 1mm x 1mm, $V_{unit}$, under an applied uniform shear stresses. Assuming that there are N of these unit volumes within a member, and the shear strengths of these, $V_{unit}$s, are randomly distributed but statistically independent. If it is also assumed that the material is perfectly brittle, then the minimum shear strength of the unit volumes represent the strength of the member. A three-parameters Weibull function can approximate the cumulative probability distribution of minimum failure shear strength with reasonably good accuracy, and has the following form:

$$w(\sigma; k, m) = 1 - e^{-\left(\frac{\sigma - \sigma_o}{m}\right)^k} \qquad \sigma \geq 0$$

$$0 \qquad \sigma \le 0$$

[12]

The three parameters in the above equation, $\sigma_o$, m, and k, are material dependent, and are typically determined experimentally. In the case of longitudinal shear strength of lumber, $\sigma$ is the shear strength, $\sigma_o$ is the minimum shear strength or the lower bound, m is the scale parameter which has the dimensions of $\sigma$, and k is the shape parameter which depends on the material. Equation 12 can be reduced into a two-parameter Weibull function by setting $\sigma_o$ to 0. This implies that lumber is capable of having zero shear strength. Although this is physically incorrect, the allowance of $\sigma_o = 0$ reduces the complexity of the analysis and provides a very good estimation for survival probability, typically 95% or greater.

In the cases considered herein, the two-parameter Weibull approximation will be used. Considering a system consisting of q unit volumes that satisfies the above assumptions of the Weibull weakest link theory, then the probability of survival (shear failure does not happen) under uniform shear stress for each unit volume is 1 minus the probability of failure, $P_f$. The probability of survival, $P_s$, can be expressed by the following:

$$P_s = 1 - P_f = 1 - (1 - e^{-(\frac{\tau^*}{m})^k}) = e^{-(\frac{\tau^*}{m})^k} \qquad [13]$$

Where $\tau^*$ denotes the uniform shear stress over the unit volume.

Let event A be the first unit volume that survives without a shear failure. Let event B be the second unit volume that survives without a shear failure and so on for all q unit volumes. The probability that all q unit volumes in the system survive without shear failure is the probability of event A intersecting event B and so on for all q unit volumes. The probability of survival, $P_S$, for each unit volume is described by equation 13. One assumes that all the events are independent of each other, then the probability of survival for the system, $P_{s(system)}$ is simply the product of each individual $P_S$. Therefore, $P_{S(system)}$ is

$$P_{s(system)} = e^{-(\frac{\tau^* 1}{m})^k} * e^{-(\frac{\tau^* 2}{m})^k} *.....e^{-(\frac{\tau^* q}{m})^k} = e^{[-(\frac{\tau^* 1}{m})^k - (\frac{\tau^* 2}{m})^k - (\frac{\tau^* q}{m})^k]}$$

When all the $\tau^*$'s are the same,

$$P_{s(system)} = e^{-q(\frac{\tau^*}{m})^k}$$

[14]

The probability of failure of the system is then

$$P_{f(system)} = 1 - P_{s(system)} = 1 - e^{-q(\frac{\tau^*}{m})^k}$$

[15]

Further, let's assume that this system of unit volumes has a total volume $\Delta V$, which equals to $qV_{unit}$, then q equals $\Delta V / V_{unit}$. Substituting this into equation 15 yields,

$$P_{f(system)} = 1 - P_{s(system)} = 1 - e^{-\frac{1}{V_{unit}}(\frac{\tau^*}{m})^k \Delta V} \qquad [16]$$

Now, consider a general system under non-uniform shear stresses. Assuming the q unit volumes are under different shear stresses ( $\sigma_i$, i= 1,2,.....q). The probability of survival of such a system can be expressed by:

$$P_{s(system,non-uniform)} = e^{-\frac{1}{V_{unit}}(\frac{\sigma_1}{m})^k \Delta V} * e^{-\frac{1}{V_{unit}}(\frac{\sigma_2}{m})^k \Delta V} \ldots\ldots * e^{-\frac{1}{V_{unit}}(\frac{\sigma_q}{m})^k \Delta V}$$

$$= e^{-\frac{1}{V_{unit}} * \frac{1}{m^k}[\sigma_1^k + \sigma_2^k + \sigma_3^k + \ldots\ldots \sigma_q^k]\Delta V} = e^{-\frac{1}{V_{unit}} * \frac{1}{m^k} \lim_{\Delta V \to 0} \sum_{i=1}^{q} (\sigma_i)^k \Delta V}$$

$$P_{s(system,non-uniform)} = e^{-\frac{1}{V_{unit}} * \frac{1}{m^k} \int_{system} (\sigma(x,y,z))^k dv_{system}} \qquad [17]$$

Where $\sigma(x,y,z)$ is a shear stress function. The probability of failure, $P_{f(system,non-uniform)}$, for the system under non-uniform shear stress is then

$$P_{f(system,non-uniform)} = 1 - e^{-\frac{1}{V_{unit}} * \frac{1}{m^k} \int_{system} (\sigma(x,y,z))^k dv_{system}} \qquad [18]$$

Now, if one equates the same probability of shear failure level, $F^*$, of the unit volume under uniform shear stresses and the general system under non-uniform shear stresses, one gets the following expression:

$$F^* = 1 - e^{-(\frac{\tau^*}{m})^k} = 1 - e^{-\frac{1}{V_{unit}} * \frac{1}{m^k} \int_{system} (\sigma(x,y,z))^k dv_{system}}$$

from which the integral parameter I can be defined as,

$$I = (\tau^*)^k = \frac{1}{V_{unit}} \int_{system} (\sigma(x,y,z))^k dv_{system}$$

$$I = \int_{system} (\sigma(x,y,z))^k dv_{system} \qquad [19]$$

In wood, brittle behaviour is common in longitudinal shear and tension perpendicular to grain, while ductile behaviour is typically observed in compression parallel and perpendicular to grain. Thus the Weibull weakest link theory is not suitable for the analysis of compression failures in wood, but was found to provide an excellent estimation for longitudinal shear strength in wood.

## 3.2 FINITE ELEMENT ANALYSIS COUPLED WITH WEIBULL WEAKEST LINK THEORY MODEL

In solving equation 19, a finite element analysis is needed to evaluate the complex shear stresses over the volume, raised to the power k. As a first attempt estimation of equation 19, a two dimensional linear elastic finite element analysis was performed, using the program FEMPC, written by R.O. Foschi (1990). An eight-noded quadratic isoparametric element was used in the analysis, which tends to converge quickly. Given an arbitrary load, boundary conditions, and the parameter k, the program returns the integration, I of equation 19, of the shear stresses over the volume for given k.

From equation 19, one can equate the integral I for a unit volume under uniform shear stresses to that of a full size beam under non-uniform shear stresses at a given probability of shear failure level. ( No integration of the shear stresses is necessary for the unit volume under uniform shear stresses). At the median level, one can rewrite equation 19 in the following way:

$$(\tau_{0.5}^{*})^{k} = \int_{beam} (\sigma(x,y,z)_{beam\ 0.5})^{k}\, dv_{beam} \qquad [20]$$

where,

$\tau_{0.5}^{*}$ = the median uniform shear stresses over the unit volume.

$\sigma(x,y,z)_{beam\ 0.5}$ = the shear stress field associated with the median shear failure load over the beam volume .

Since FEMPC is a linear elastic model, the following expression holds,

$$\frac{\sigma(x,y,z)_{beam}}{P_{beam}} = \frac{\sigma(x,y,z)_{input}}{P_{input}} \qquad [21]$$

where,

$\sigma(x,y,z)_{input}$ = the shear stress field associated with the input load $P_{input}$ for the program FEMPC.

$\sigma(x,y,z)_{beam}$ = the shear stress field associated with the load $P_{beam}$ of the beam in question.

Let

$$I_{beam} = \int_{beam} (\sigma(x,y,z)_{beam})^k dv \qquad [22]$$

then substituting equation 21 into equation 22, yields the following:

$$I_{beam} = \int_{beam} \left[ P_{beam} \left( \frac{\sigma(x,y,z)_{input}}{P_{input}} \right) \right]^k dv$$

$$= \left[ \frac{P_{beam}}{P_{input}} \right]^k \int_{beam} (\sigma(x,y,z)_{input})^k dv \qquad [23]$$

and letting,

$$I_{input} = \int_{beam} (\sigma(x,y,z)_{input})^k dv \qquad [24]$$

therefore equation 23 becomes

$$I_{beam} = \left[ \frac{P_{beam}}{P_{input}} \right]^k I_{input} \qquad [25]$$

One can substitute equation 25 and 22 into 20 and hence

$$P_{beam\ 0.5} = \frac{(\tau^{*}_{0.5})(P_{input})}{[I_{input}]^{k}} \qquad [26]$$

where $P_{beam\ 0.5}$ is the median beam failure shear load.

Given the median uniform failure shear stresses over a unit volume, $\tau^{*}_{0.5}$, the Weibull shape parameter k for that material, and obtaining $I_{input}$ from an arbitrary input load $P_{input}$ (*from the program FEMPC*), a prediction of the median failure load for the beam is possible using equation 26.

It is physically very difficult to obtain the value of the uniform stresses, $\tau^{*}$, over a unit volume. Thus an estimation is necessary. Based on finite element and regression analyses on existing ASTM shear block data, Barrett and Foschi (1975) related ASTM shear block results to the uniform stresses over the unit volume for several cases of different k values. They suggested that the uniform stress, $\tau^{*}$, over the unit volume is

$$\tau^{*} = \tau_{ASTM}\,\beta_t \qquad [27]$$

where,

$\tau_{ASTM}$ = Shear stresses for the ASTM shear block.
$\beta_t$ = $1.33 + 0.336\,(k - 4)$ if $4 \leq k \leq 8$

$\beta_t = 2.678 + 0.251\,(k - 8)$ if $8 \le k \le 10$

If $P_{ASTM}$ is the load applied to the ASTM shear block, then $\tau_{ASTM}$ is defined as the average shear stress over the shear area $A_s$ ;

$$\tau_{ASTM} = \frac{P_{ASTM}}{A_s} \qquad [28]$$

Based on the ASTM shear block test results, the shear strength of the unit volume can be estimated using equation 27. The Weibull shape parameter k can be fitted to the ASTM shear block results or can also be conveniently estimated as (Leicester, 1991)

$$k = CV^{-1.085} \qquad [29]$$

where

$CV$ = coefficient of variation of shear strength.

Equation 19 can be solved for any desired probability of survival by entering an arbitrary input load into FEMPC. The program will give the corresponding I, which can then be entered into equation 26.

Based on classical engineering mechanics theory and assuming point loads and simple supports, the magnitude of the shear forces in the middle spans are 2.2 times the shear forces in the end spans (see Figure 15). The maximum shear stresses, $\sigma_{max\ classical}$ can be estimated as:

$$\sigma_{max\ classical} = \frac{33\ P}{64\ bd} \qquad [30]$$

where

P = total maximum load,
b = beam width, and
d = beam depth.

Note that the shear stress calculated from the classical theory is independent of test span to specimen depth ratio. The predicted failure shear stresses of a beam can be estimated using equation 30 with the predicted failure shear load evaluated using the general form of equation 26 at any given level of probability of failure.

# 4. EXPERIMENTAL STUDY

## 4.1 MATERIAL

Three species groups of Canadian softwood dimension lumber were sampled from mills in British Columbia: Douglas-Fir, Hem-Fir, and Spruce-Pine-Fir. Approximately 100 pieces of nominal 38 mm x 185 mm x 3 m lumber were obtained for each species group. Due to availability at the time of this study, only nominal 38 mm x 285 mm x 4.87 m of Hem-Fir and Spruce-Pine-Fir were used. Again, the sample size was approximately 100 pieces for each species groups. The material was kiln dried and conformed to be Select Structural grade. After delivery to the laboratory, the specimens were further air dried to an equilibrium moisture content of approximately 12%.

## 4.2 FLAT-WISE MODULUS OF ELASTICITY

A Cook Bolinders AG-SF grading machine was used to measure the flat-wise modulus of elasticity (MOE) profile along each specimen's length. It was checked for accuracy at the beginning of each test day. An aluminum bar with a known flat-wise MOE was fed into the Cook Bolinders AG-SF grading machine. Five readings were read from each side of the bar and the average was compared against the known MOE value. No adjustments were necessary if the

readings fell within 10 % of the known value. Once the machine was calibrated, full length specimens were fed through the machine lengthwise with the grade stamp end first.

The specimens were hand pushed into the mouth of the machine on level infeed roller tables with a speed approximately equal to the infeed speed of the moving rollers inside the machine. The specimens were guided gently by hand as they moved through the rollers to avoid vibrations that could effect the accuracy of the load readings. Infeed roller tables were necessary on both ends of the machine to ensure the specimens were level during the entire pass through the machine. The Cook Bolinders AG-SF grading machine has photo cell sensors at the mouth of the machine and after the second set of rollers, C1 and C2. Figure 3 shows a schematic diagram of the Cook Bolinders' working mechanisms. As a specimen passes through the photo cell sensor, rollers A1 and A2 clamp onto the specimen and start to feed it into the machine. The feeding system moves the specimen into the rollers at a rate of 0.508m/sec. The machine's load sensor (located behind roller B in Figure 3) waits for a prescribed amount of time which corresponds to the time necessary for the specimen to reach the rollers C1 and C2 before it starts recording the load. Once the end of the specimen reaches the photo cell sensor for the second time, the machine stops recording. Thus the load profile begins and ends with a margin of 500 mm of no data on both ends of each specimen. The Cook Bolinders AG-SF grading machine then waits to record the same specimen again. Each run requires two passes of the same piece. The specimen was then rotated 180° about its longitudinal axis and fed through the machine again. The load profiles from both passes were averaged to eliminate the effects of bow and surface roughness of the specimen. Figure 4 shows the machine in the process of testing a specimen. The rollers inside the machine simulated a simple three point loading condition. The specimens were deflected on flat

under center point loading on a span of 900 mm with a prescribed center point deflection of 4.5 mm.

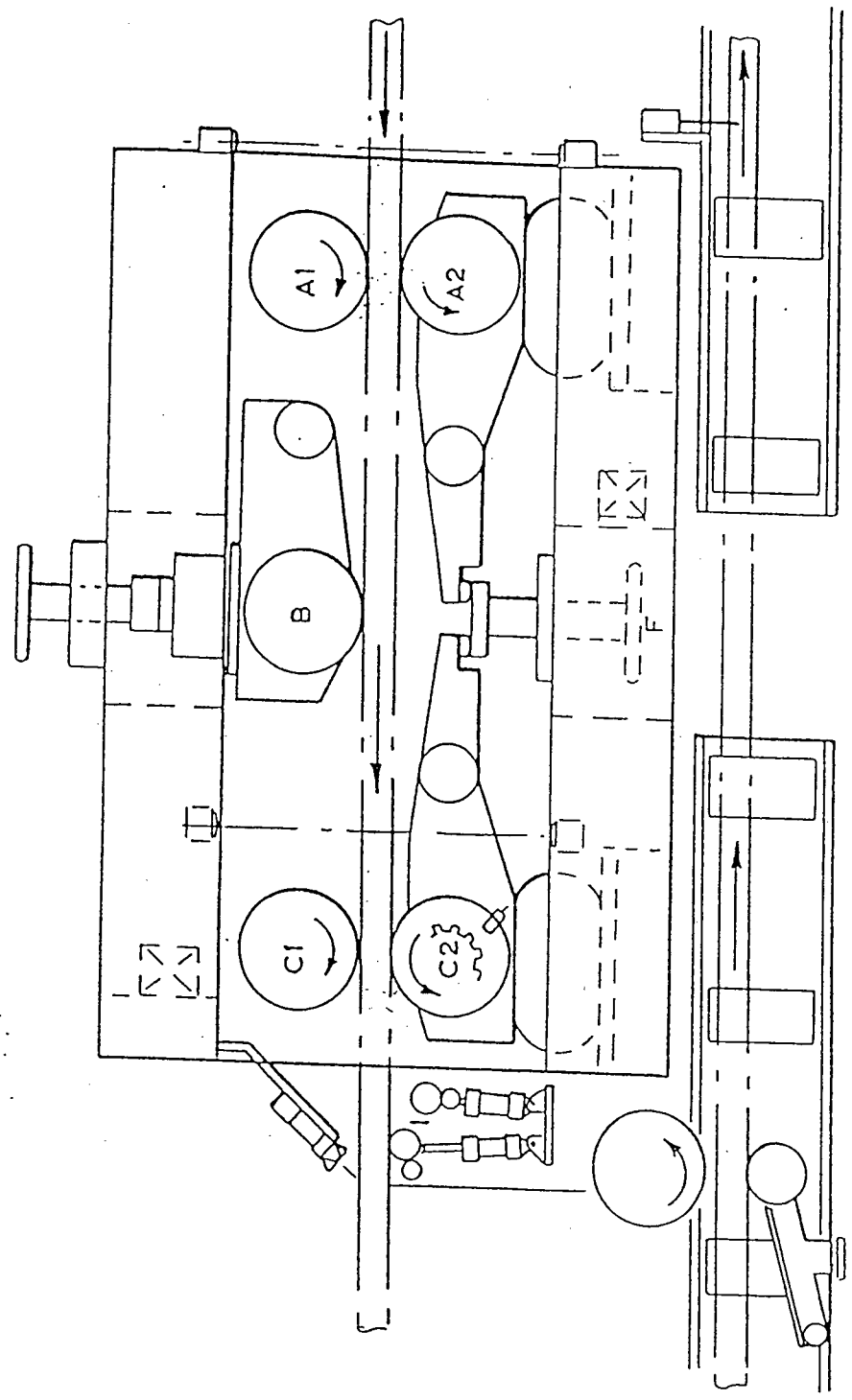


Figure 3. Sequence description of the Cook Bolinders AG-SF grading machine

This 4.5 mm displacement was large enough to produce a reasonable MOE profile and yet small enough to prevent any destructive bending failures. The force required to deform the specimens was continuously monitored and later converted into flat-wise MOE estimates.

The deflection of the simulated simple three point loading from the three rollers can be expressed as:

$$\Delta = \frac{PL^3}{48 E_{flat} I_y} \qquad [31]$$

where,

$\Delta$ = deflection at center
P = load
L = span between the center of the outer rollers
$E_{flat}$ = flat-wise modulus of elasticity (MOE)
$I_y$ = moment of inertia. For a rectangular beam section on flat, it has the following form:

$$I_y = \frac{bh^3}{12} \qquad [32]$$

where,

b = depth of the beam.
h = thickness of the beam.

Equation 31 can easily be rearranged to

$$E_{flat} = \frac{PL^3}{48 \Delta I_y} \qquad [33]$$

for the evaluation of the flat-wise MOE ($E_{flat}$).

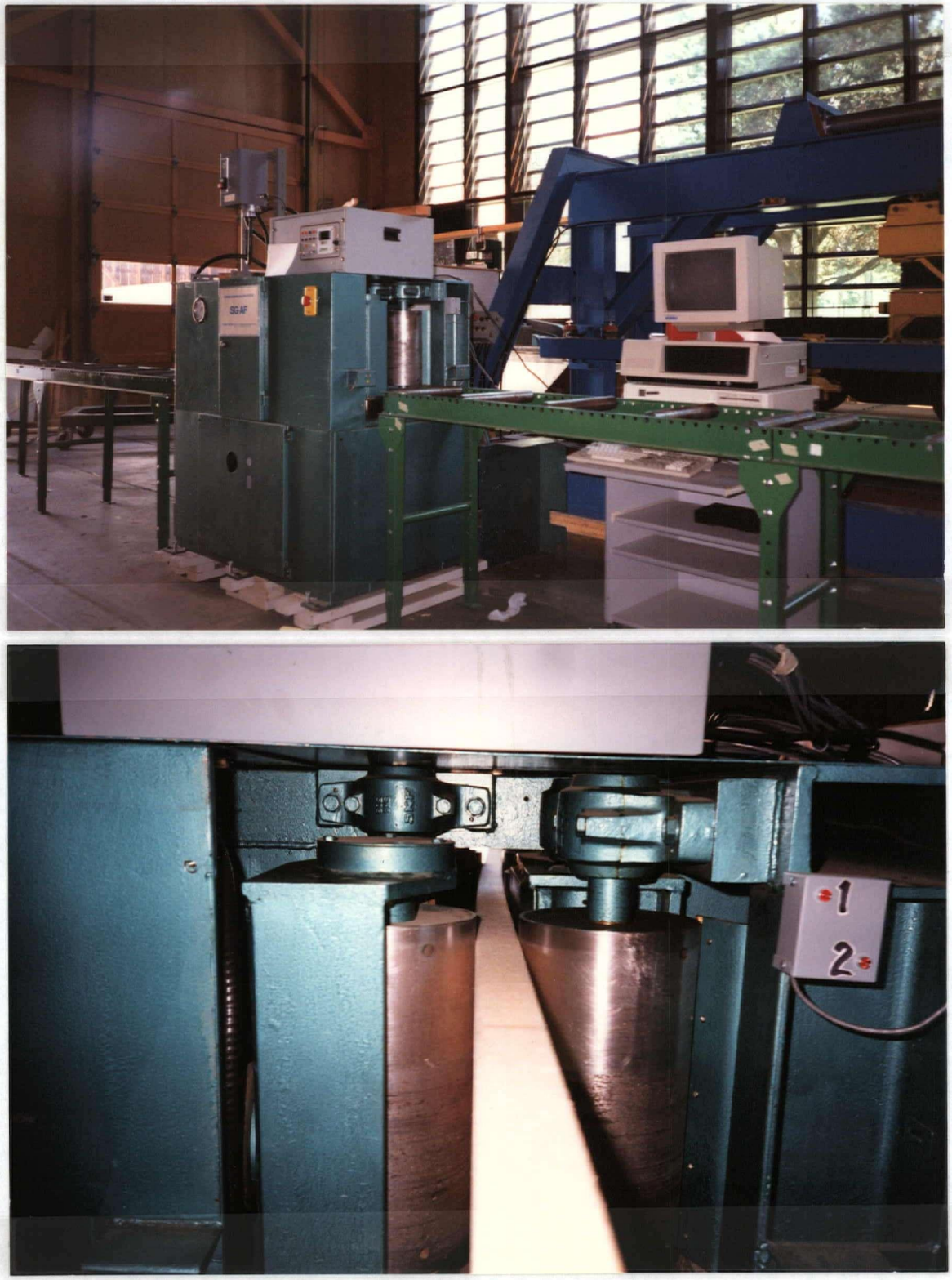


Figure 4. Cook Bolinders AG-SF grading machine

## 4.3 EDGE-WISE MODULUS OF ELASTICITY

A 224 kN capacity bending machine was used to measured the edge-wise MOE of full size specimens under a standard four point bending configuration. Figure 5 shows the span and locations of the loading heads of the machine. Two different spans were used in this test. A total span of 2.96 m was used for all the 38mm x 185mm specimens and a span of 4.845 m was used for the 38mm x 285m specimens. The end reactions and loading heads were 15 cm long by 10 cm wide. A hydraulic actuator was used to move the loading heads with a maximum stroke of 254 mm. The reaction and loading heads were pivoted to simulate roller type reactions. Lateral supports prevented out-of-plane buckling of the specimens.

A yoke device with a linear variable differential transformer (LVDT) was used to measure the beam's mid-depth displacement relative to a line joining points A and B on top of the loading heads (Figure 5). The stroke displacements of the actuator, the yoke displacement, and the applied load were recorded at regular intervals by data acquisition software on a personal computer. A real time display of the loads versus actuator's and yoke's LVDT measured displacements were used as guide to discontinue loading when enough points were collected. The maximum load for each specimen was set at 3 kN with a rate of loading of 0.5mm/s. The average time of loading for each specimen was under one minute.

Using elementary principles of mechanics of materials, the yoke's displacement at C in Figure 5 can be estimated by:

$$\Delta_c = \frac{PL^3}{432 E_{edge} I_x} \qquad [34]$$

where,

$E_{edge}$ = edge-wise Modulus of Elasticity (MOE)
$P$ = applied load
$\Delta_c$ = displacement measured by the yoke's LVDT at point C relative to line AB.
$L$ = span between the two supports
$I_x$ = moment of inertia for the rectangular beam about the strong axis.
$= \frac{1}{12} b^3 h$

Equation 34 can be rearranged in the following form:

$$E_{edge} = \frac{PL^3}{432 \Delta_c I_x} \qquad [35]$$

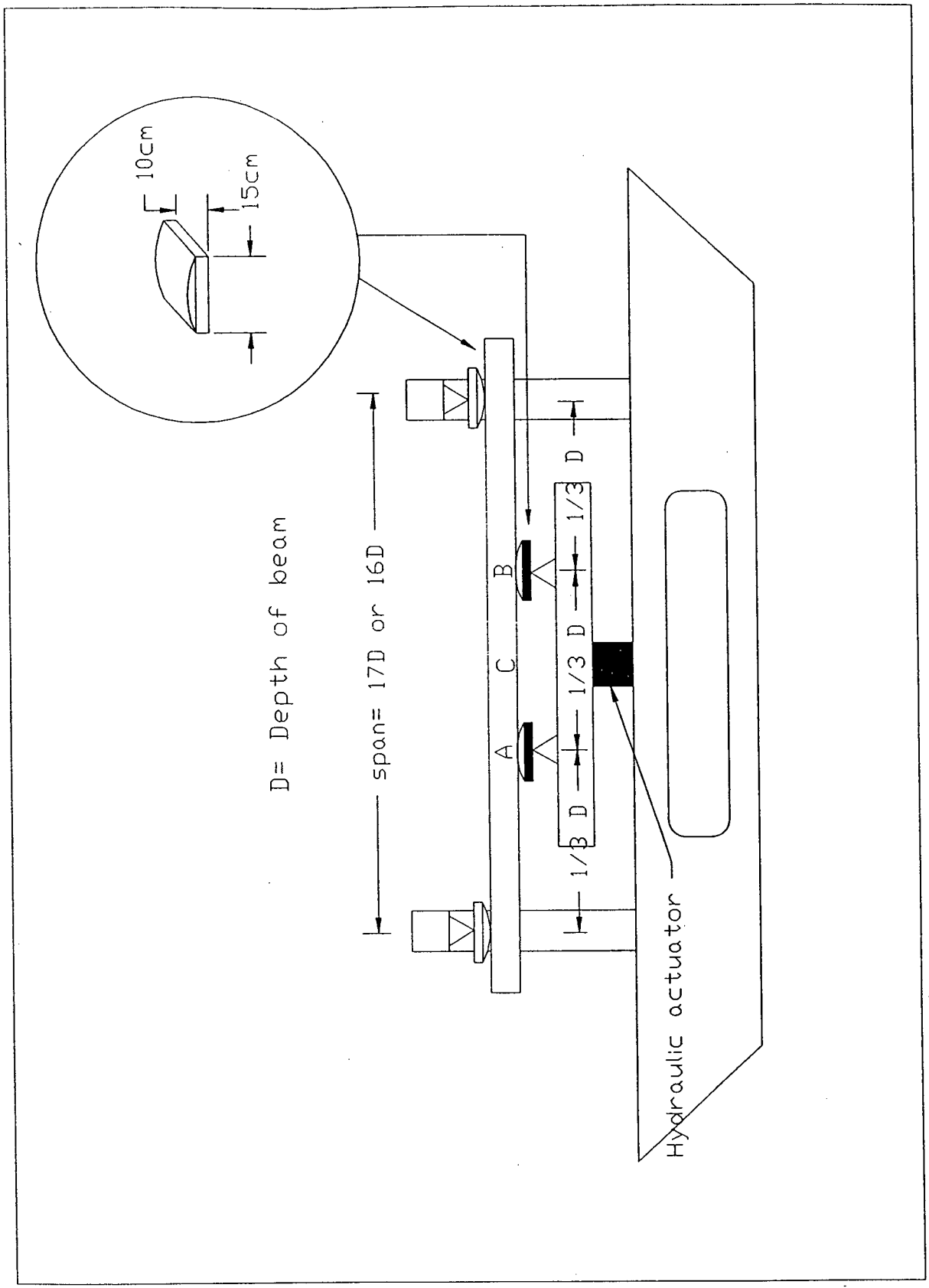


Figure 5. 224 kN Bending Machine

## 4.4 LONGITUDINAL SHEAR TESTS.

A modified Tinius Olsen Universal testing machine with 889kN capacity was used for the full size longitudinal shear test. The loading head was controlled vertically with mechanical gears selected at low speed. Figure 6 shows the Tinius Olsen machine in the Civil Engineering Structures laboratory. The two span five point bending shear test configuration, with specimen depth to span ratios of 5:1 (5D) and 6:1 (6D) is shown in Figure 7. Because bending failures typically dictate the load carrying capacity of beams, a special loading arrangement was required that produced a high shear-to-bending failure ratio. Experience has shown that 5 point bending tests can produce a greater percentage of shear failures compared to other full size bending shear tests. The shear to bending stress ratio, $\sigma_{shear}/\sigma_{bending}$, is higher in the 5 point bending test than the conventional four point bending test. To produce the shear stresses necessary to fail the members, the high load levels could cause compression perpendicular to grain failures to become a serious concern. Special care was needed in designing the reactions and loading heads to minimize crushing of the wood.

The design of the loading heads and the reaction plates had to be large enough to avoid extensive compression perpendicular to grain failures. A compression perpendicular to grain test was conducted in establishing the compressive strength of the softest species at hand which was Spruce-Pine-Fir. Twenty-five blocks, 100mm x 100mm x 38mm, were randomly cut from the group of nominal 38mm x 285mm Spruce-Pine-Fir for the test. The mean moisture content of these blocks was 15 % with a mean green specific gravity of 0.42. The mean compression strength perpendicular to grain for all 25 specimens was 1.8 MPa.

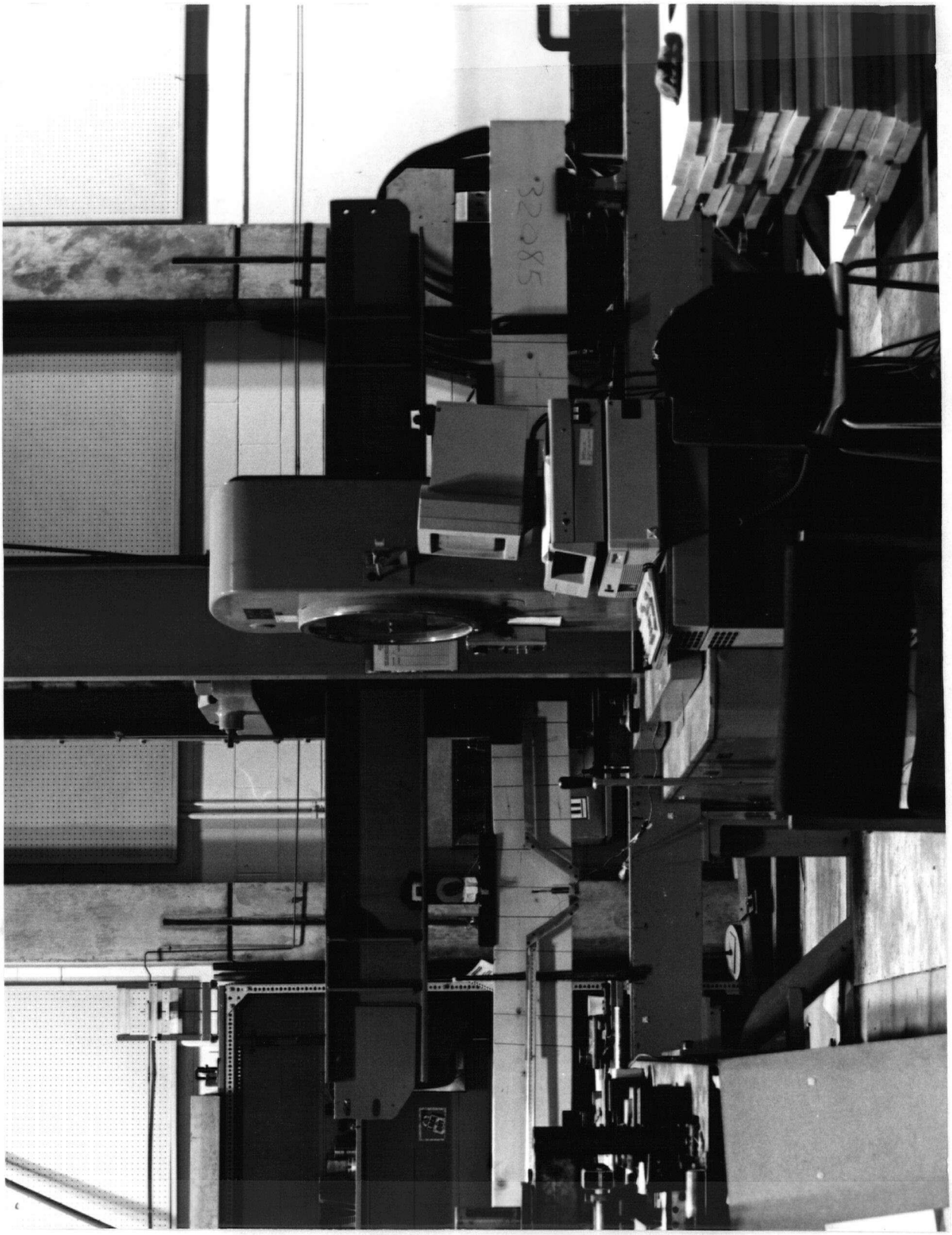

Figure 6. Tinlus Olsen two span five point bending machine

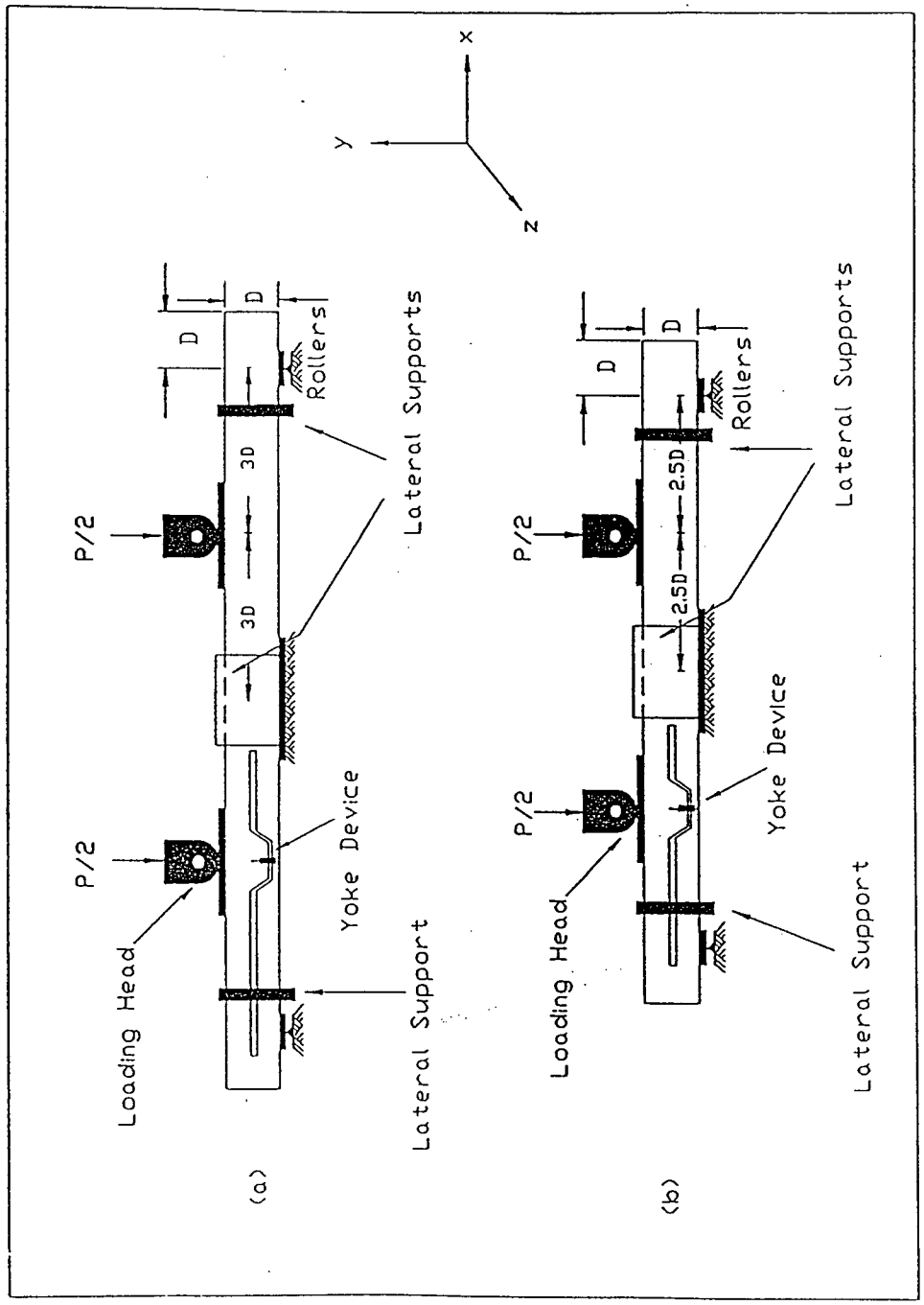


Figure 7. Two span 5 point bending test configurations 5D and 6D

For the nominal 38mm x 185mm beams in both the 5D and 6D configurations, the loading head plates were designed to be 336 mm in length parallel to the longitudinal direction of the beams. The center and end reactions were 420mm and 120 mm respectively. For the nominal 38mm x 285mm beams, the initial loading head plate size was 400 mm for both species and both configurations. Figures 8.1 to 8.6 show the finite element meshes for half of the beam (symmetric over mid-length) and the reaction plate sizes for all sample groups.

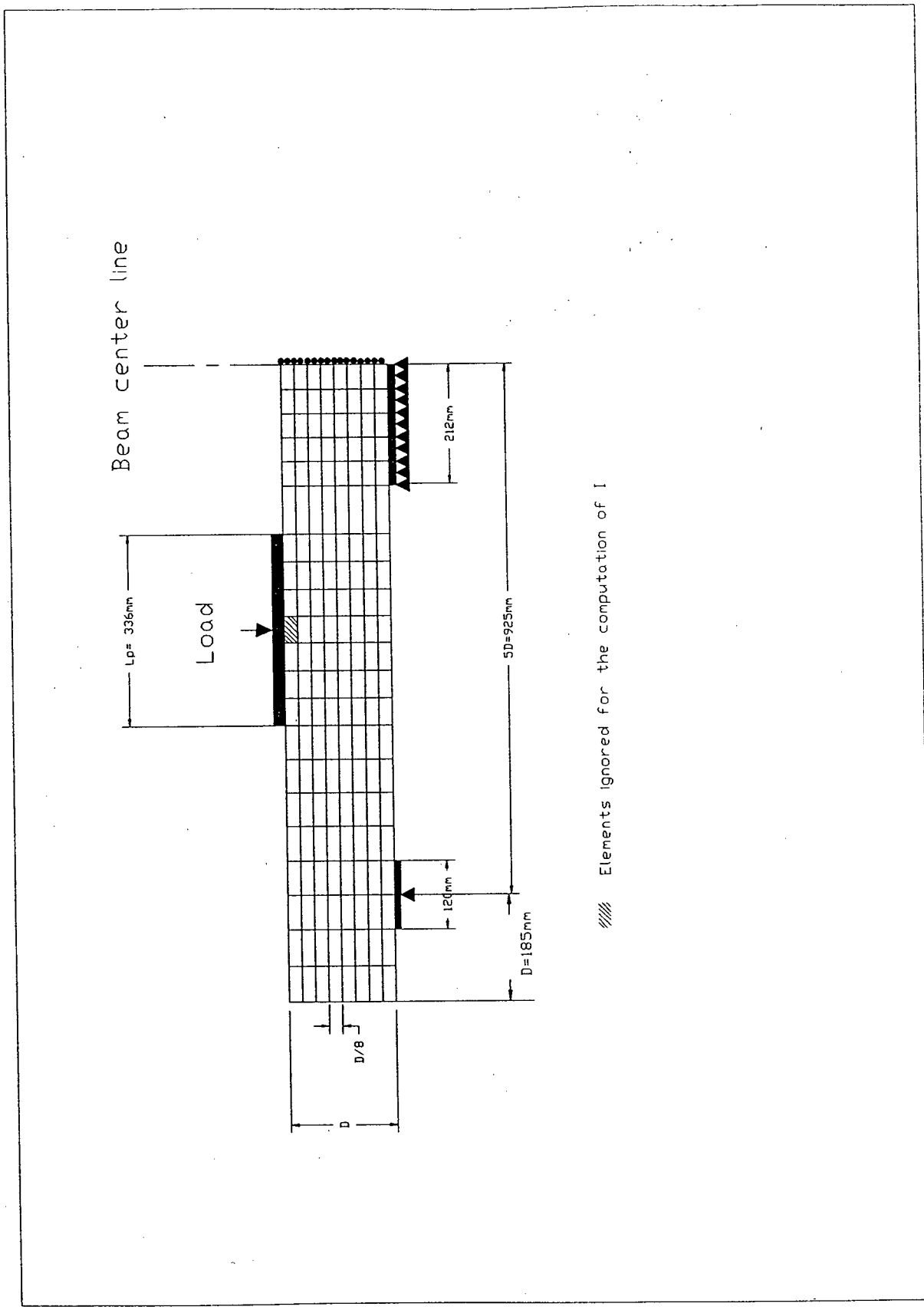


Figure 8.1 Finite element mesh about the mid span for span to depth ratio of 5:1 (38mmx185mm)

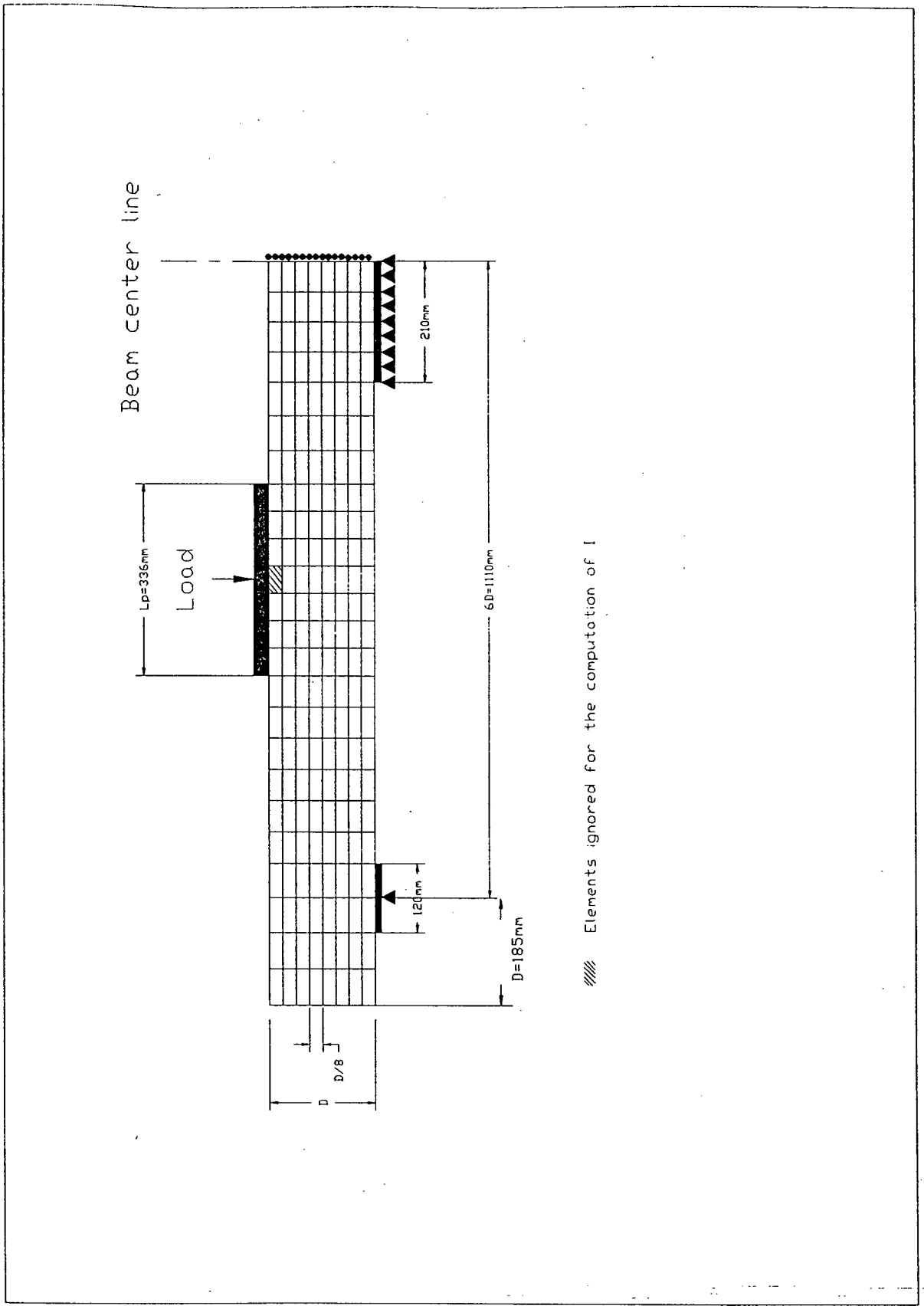


Figure 8.2 Finite element mesh about the mid span for span to depth ratio of 6:1 (38mmx185mm)

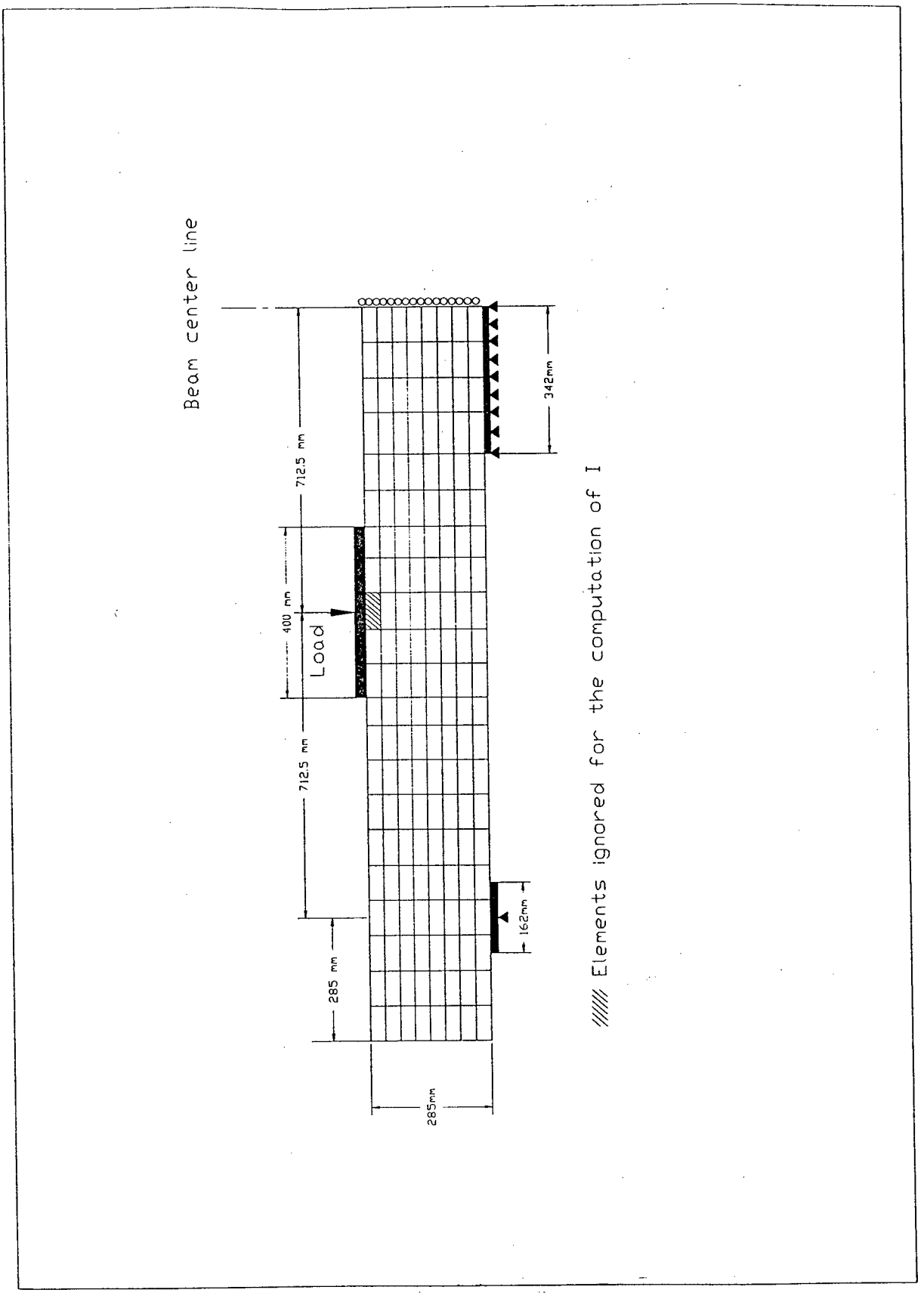


Figure 8.3 Finite element mesh about the mid span for span to depth ratio of 5:1 (38mmx285mm) S-P-F

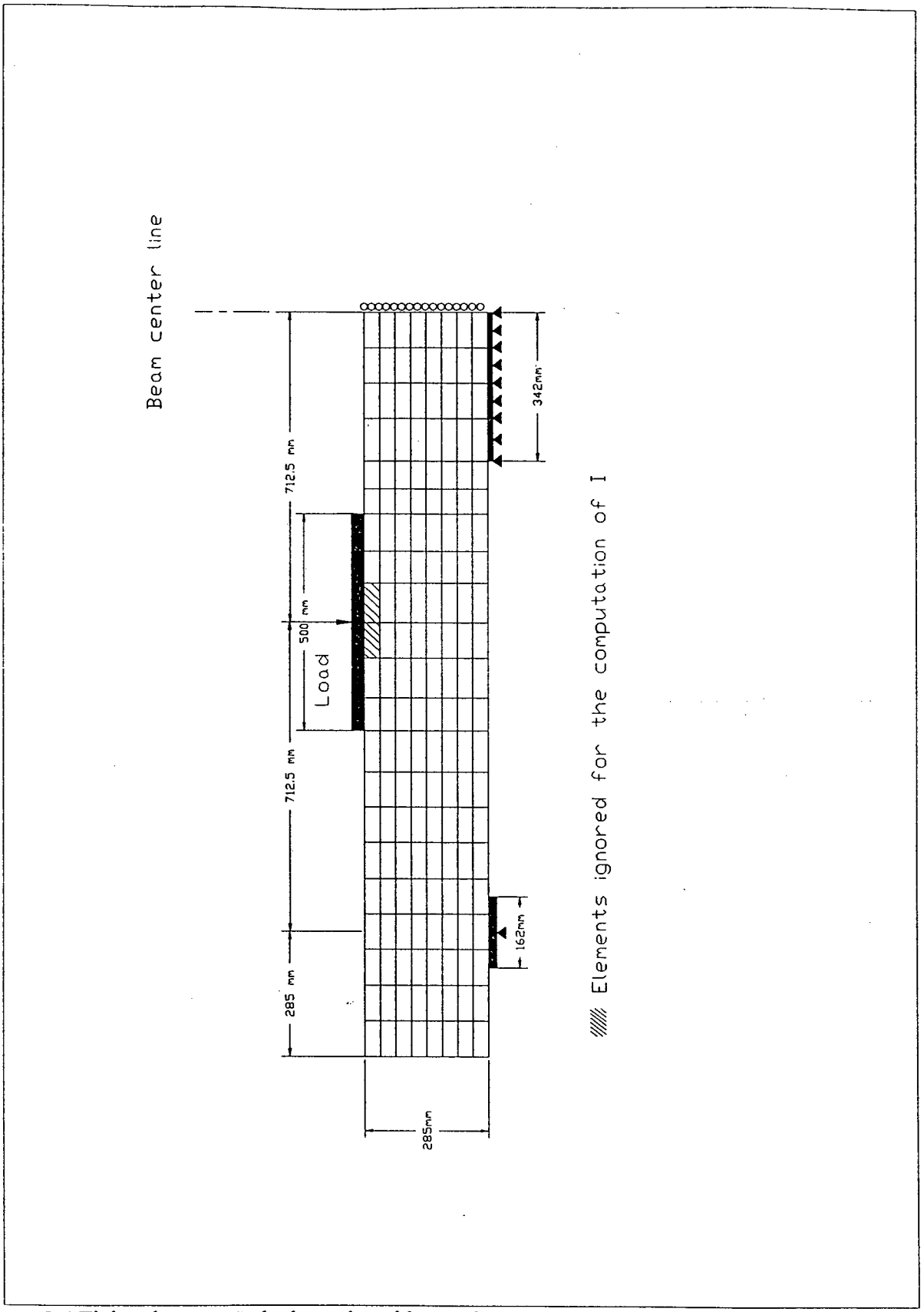


Figure 8.4 Finite element mesh about the mid span for span to depth ratio of 5:1 (38mmx285mm) H-F

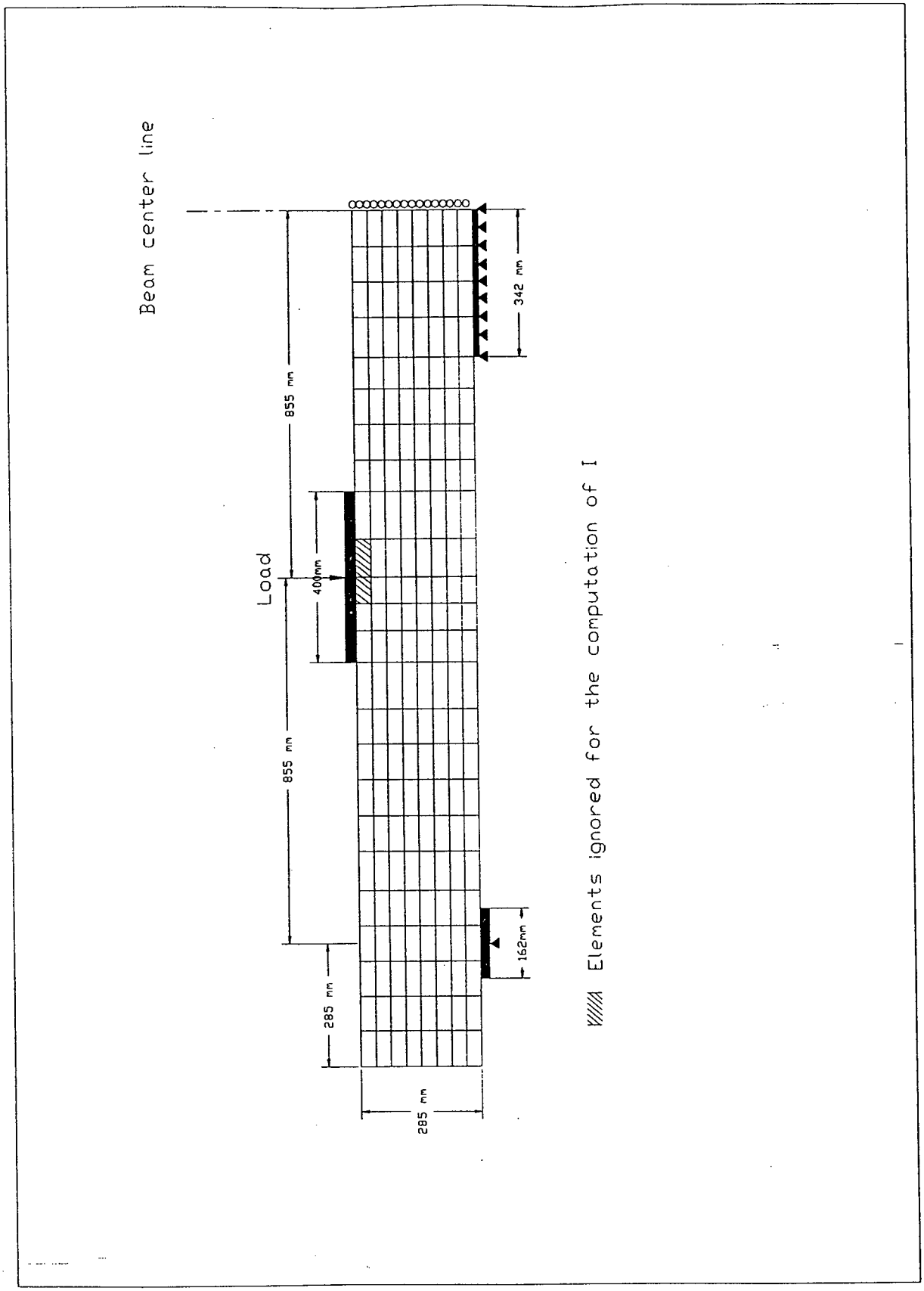


Figure 8.5 Finite element mesh about the mid span for span to depth ratio of 6:1 (38mmx285mm) S-P-F

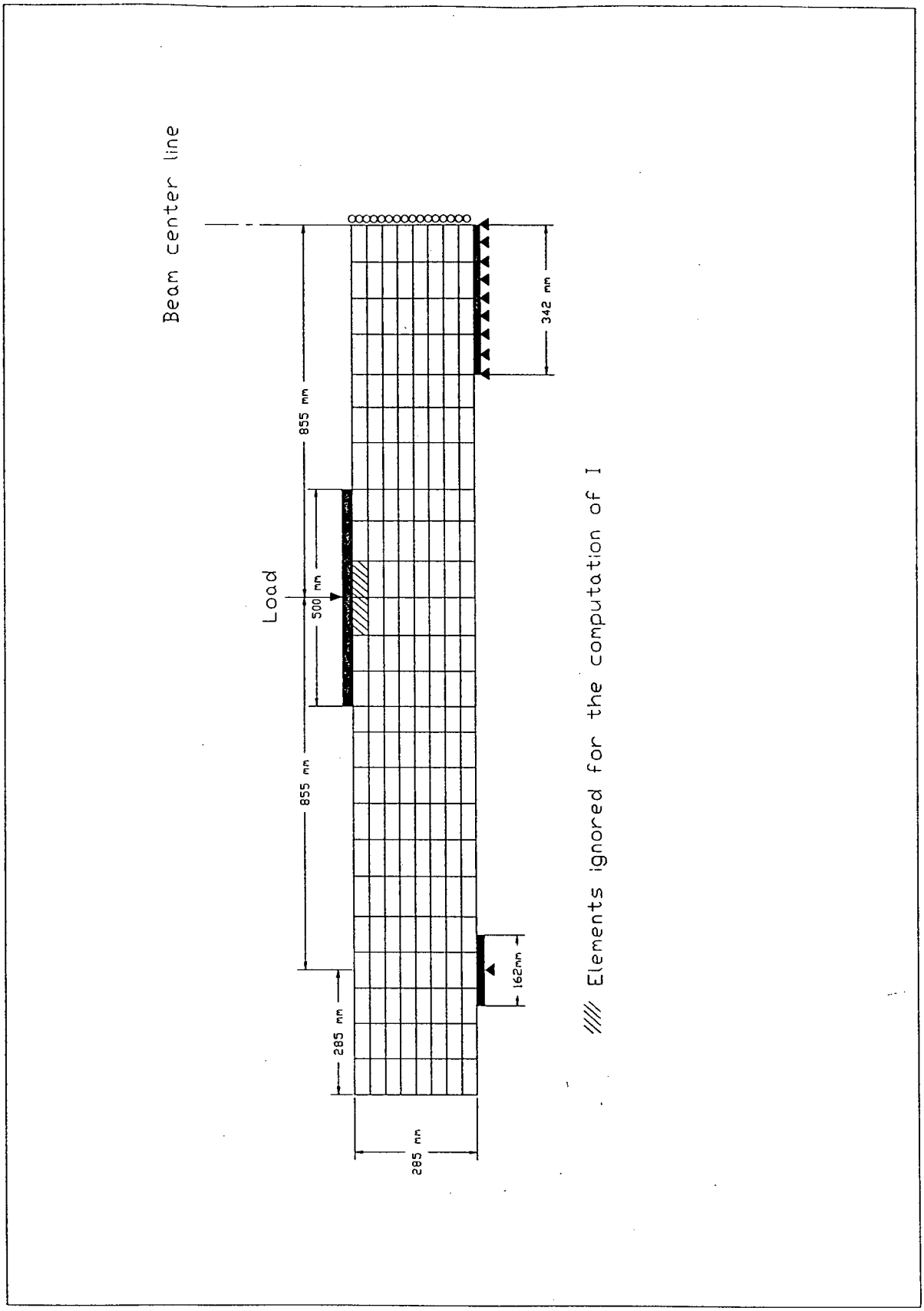


Figure 8.6 Finite element mesh about the mid span for span to depth ratio of 6:1 (38mmx285mm) H-F

The center and end reactions were 684 mm and 163 mm respectively. The width for all plates was 100 mm. Using this plate size initially on the Spruce-Pine-Fir resulted in frequent compression perpendicular to grain failures and a new loading plate size of 500 mm was later used on the Hem-Fir (compromising with a shorter span).To be consistent, the 400 mm plate was continued to be used throughout for the Spruce-Pine-Fir group.

The thickness of the loading heads and reaction plates in all cases were approximately 60 mm and 30 mm thick respectively to ensure that they remain rigid to distribute the loads evenly onto the beams. The loading heads were attached to an I-beam 350 mm deep to ensure loading was evenly distributed to each loading head.

The two end reactions and the loading heads were allowed to rotate about the z-axis (see figure 7). This simulated a pinned type support. The center support remained fixed. Lateral supports were in place between the loading heads and end reactions. In this region lateral buckling would most likely occur. Special care was taken to ensure the lateral supports did not produce an unacceptable amount of friction which might affect the stresses in the beam. Teflon pads were placed between the beam's surface and the lateral supports. Lateral supports were also in place at the center reaction. All lateral supports extend beyond the depth of the beam.

One LVDT was attached to the I-beam to measure the displacement of the loading heads, while another LVDT was attached to the beam on a yoke. This LVDT, located under one of the loading heads, was used to measure the displacement at mid-depth of the beam relative to the center support and the end reaction. This measured displacement was used as a check against the

finite element analysis results. Randomly selected values showed good agreement with the finite element predictions.

The accuracy of the mechanical Tinius Olsen load display was checked against a calibrated electronic load cell. The load readings from the Tinius Olsen was within 2% from that of the load cell.

An overhang, equal to the member depth, measured from the center of the end reaction plate, was provided at each end of the member. The specimens for the full size shear test were trimmed to eliminate excessive overhang in such a way to avoid end cracks in the members. Any members with cracks or end splits that could not be trimmed to provide the proper length were rejected from the test. Once the members were trimmed, they were transported from the storage site into the laboratory for testing in groups of thirty. Each piece was further inspected before the actual shear test to ensure the member was free from end splits or cracks. Vertical lines, at an approximate spacing of 30 mm were drawn on both wide faces of each specimen which served to detect longitudinal shear failures. The average loading rate was 5 mm/min. This conforms to the ASTM D 198 (1994b) which specifies maximum load to be attained between 6 and 20 minutes. The load and both displacements were recorded by a computer controlled data acquistion system. The load was also monitored from the dial type display and was manually recorded as a back-up. A real time display of the load versus the loading head displacement was available. From this display, it was easy to determine any failure by the sudden drop in load. A typical load-deflection curve is shown in figure 30 of appendix B. The location and types of failures were also recorded. Once the member had failed, the loading heads were kept in position. This allowed a careful

examination of the failure mode at the time of failure for classification. Figure 9 shows the different failure modes and their classifications encountered during the testing program. Photographs were taken for each specimen after failure. In some cases, failures in the shearing mode were not readily apparent. A rule was adopted that if failures resulted in cracks or splits which extended within 25 mm of the top and bottom surfaces of the beam, these beams were not considered as failures in shear, and were attributed to tension type failures because shear stresses in these regions were expected to be reasonably low.

## 4.5 SHEAR BLOCK TESTS

An ASTM shear block (ASTM D143) with dimensions as shown in Figure 10 was obtained from each of the failed specimen. They were defects free and of straight grain. All the surfaces were cut as plane and at right angle to each other as possible, to minimize any possible eccentric loading during the shear block test. A standard shear test apparatus was used for the ASTM shear block test. A MTS 810 Material Test System was used to control the ramp movement and rate of loading (15.24 mm/min). The maximum allowable displacement of the shearing plane was ± 7.62 mm. The capacity was set at 50,000 N. A real time display of load versus displacement was available. A sudden drop in load was an indication that the block had failed. The average time to failure was between 5 and 10 minutes. A personal computer was used to record the loads at a sampling frequency of 2 Hz. Dimensions of the shear planes were measured and recorded manually just before the shear test. These data were used later to determine the average shear stresses within the shearing plane of each block.

a)

b)

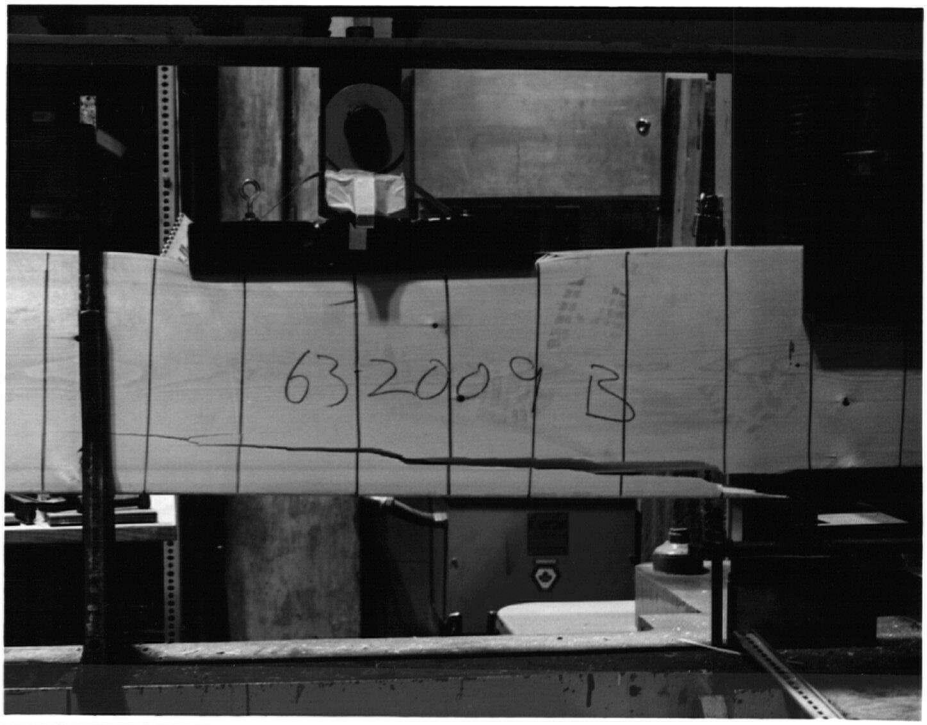


Figure 9. Different modes of failures in the two span five point bending test: (a)shear failure, (b)tension perpendicular to grain failure

c)

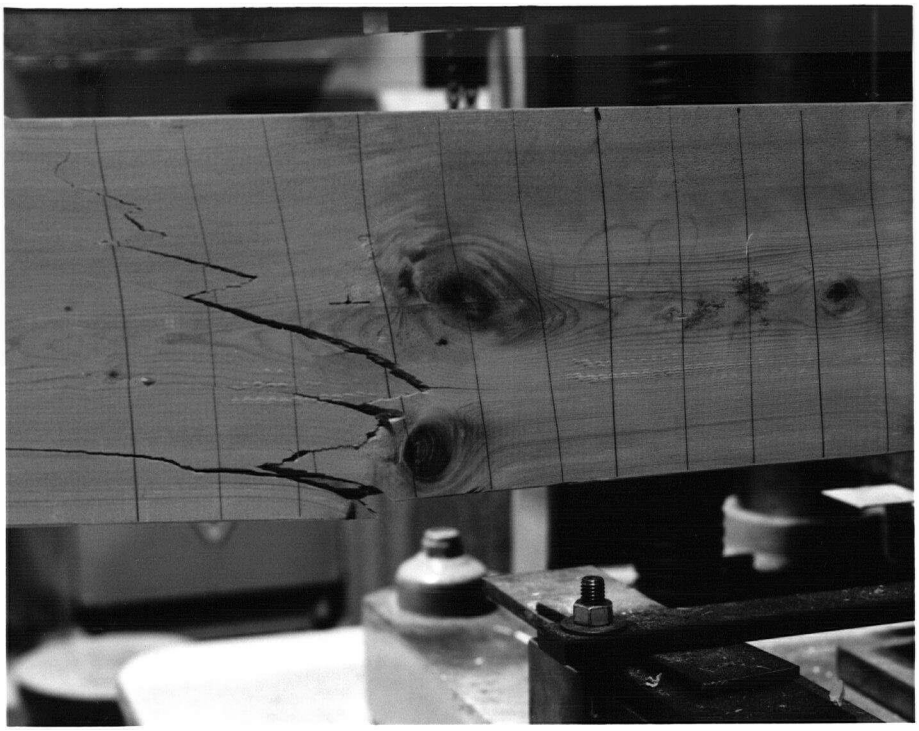

d)


Figure 9. Different modes of failures in the two span five point bending test: (c) bending failure, (d) compression failure

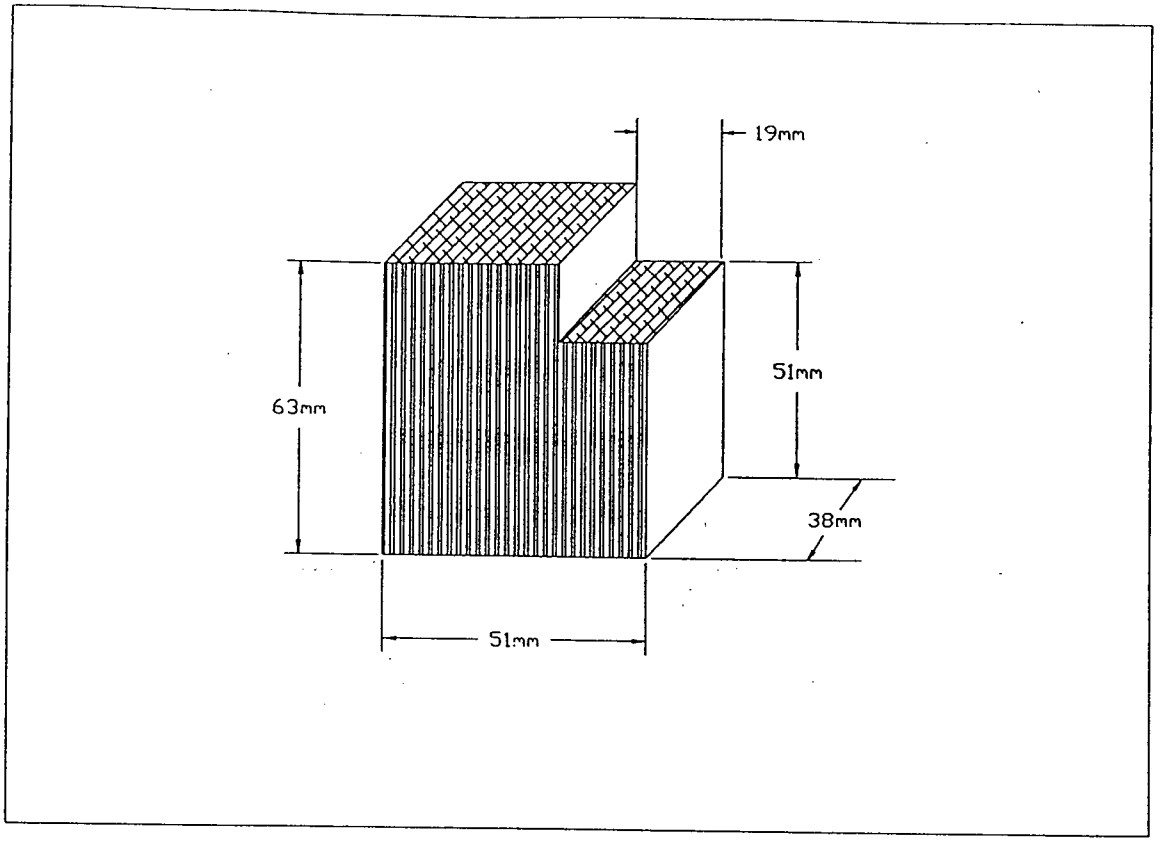


Figure 10. ASTM shear block

## 4.6 SPECIFIC GRAVITY TEST

Blocks with nominal dimensions 38mm x 63mm x 51mm were extracted from failed specimens for specific gravity tests. The exact green dimensions and weights were manually measured using a digital caliper, accurate to 1/100 of a mm. Once the blocks were measured and weighed, they were oven-dried under a constant temperature of 103 °C for 24 hours. The blocks were then taken out, one batch at time. The dry dimensions and weights of the blocks were measured once more when the blocks were cool to the touch.

# 5. RESULTS AND DISCUSSION

## 5.1 MODULUS OF ELASTICITY ESTIMATION

The load profiles from both sides of the beam, obtained from the Cook Bolinders AG-SF grading machine, were further superimposed to obtaine a single average load profile. This was later converted to a flat-wise modulus of elasticity (MOE) profile using equation 33. A single average value was then obtained from this flat-wise MOE profile. The results for both nominal 38mm x 185mm and 38mm x 285mm of the different species are listed in Tables 1 and 2.

The estimation of the edge-wise MOE was based on equation 35. A linear regression was performed on a selected range of points free from outliers for the estimation of the ratio, $P/\Delta$. It is not uncommon to get outliers at the beginning of the test when the loading heads first make contact with the beam. However, once the loading heads have settled down, the relationship between P and $\Delta$ becomes fairly linear.

It was observed that, in general, the nominal 38mm x 185mm Hem-Fir specimens had an unusual amount of large knots for a supposedly select structural grade. Both the flat-wise MOE and edge-wise MOE were lower than the nominal 38mm x 285mm Hem-Fir specimens which were mainly clear materials.

Figure 27 in appendix B shows a typical relationships between the edge-wise MOE and beam failure shear stresses. Figure 29 shows a typical relationships between the edge-wise MOE and the ASTM shear block shear strength. The $R^2$ values from a simple linear regression analysis range between 0.00 and 0.32 for all species and nominal sizes, and suggest very little linear correlation exists between the above relationships.

## 5.2 ASTM SHEAR BLOCKS RESULTS

ASTM shear block tests were conducted on each beam regardless of the beam's failure mode. The shear strength was estimated by equation 28. Tables 9 and 10 show the median and 5th percentile ASTM shear strengths of the different species for nominal 38mm x 185mm and 38mm x 285mm respectively. ASTM shear block shear strengths from the two different nominal sizes but of the same species, exhibit similar values. A two-parameter Weibull fit was conducted for the determination of the 5th percentile shear strength of the ASTM shear block. Once the two parameters m(scale), and k(shape) were determined, the 5th percentile shear strength estimation, $\sigma_{0.05}$, for a fairly large sample size could be evaluated by the following:

$$\sigma_{0.05} = m\left[\ln\left[\frac{1}{1-0.05}\right]\right]^{\frac{1}{k}} \qquad [36]$$

The median and 5th percentile shear strength of ASTM shear blocks and the fitted k values were later used for the prediction of the full size beam failure shear load.

## 5.3 SPECIFIC GRAVITY RESULTS

Tables 1 and 2 show the median oven dry specific gravity results for the different species and nominal sizes. The oven dry specific gravity, $SG_{oven\ dry}$ was calculated using the following equation:

$$SG_{oven\,dry} = \frac{WT_{od}}{V_{od}\rho_w} \qquad [37]$$

where,

$WT_{od}$ = oven dry weight of the blocks
$V_{od}$ = oven dry volume of the blocks
$\rho_w$ = density of water = 0.001 g/mm$^3$

The median specific gravity of blocks from the same species but of different nominal sizes did not exhibit a significant difference. Figures 26 in appendix B shows the typical relationship between the oven dry specific gravity and beam failure shear stresses. Figure 28 shows the typical relationship between $SG_{oven\ dry}$ and the shear strength of the ASTM shear blocks. Again, the $R^2$ values which range between 0.05 and 0.52 suggest no strong linear correlation for the above relationships.

## 5.4 FULL SIZE BEAM RESULTS

Linear elastic finite element analyses, using eight-noded quadratic isoparametric elements, were performed to determine the stress distributions in the two test configurations. Figure 8.1 to 8.6 show the finite element meshes chosen for the analyses with symmetry about mid-span taken into consideration.

The MOE perpendicular to grain and the shear modulus that were used in the analysis were estimated for softwood (Bodig and Goodman, 1973) by the following:

$$\log E_{perd} = \log(5.2140) + 0.6749 \log(E_{edge}) \quad [38]$$

$$\log G = \log(3685.2) + 0.23585 \log(E_{edge}) \quad [39]$$

where

$E_{perd}$ = modulus of elasticity perpendicular to grain in psi
$E_{edge}$ = edge-wise modulus of elasticity in psi
G = shear modulus in psi

The modulus of elasticity values in the x and y directions, modulus of rigidity, and Poisson ratios ($\nu_{xy}$ and $\nu_{yx}$) of the three species and two sizes used in the finite element analyses are given in Tables 7 and 8. Here the x and y directions are taken as the direction parallel and perpendicular to the long axis of the member, respectively.

Since the values of Poisson ratio, $\nu_{xy}$ (strain perpendicular to grain due to stresses along the grain), and $\nu_{yx}$ (strain along the grain due to stresses perpendicular to grain) are very small for wood and also very difficult to measure, an estimated average value of $\nu_{xy}$, and $\nu_{yx}$ for softwood of 0.42 and 0.033 (Bodig and Goodman, 1973) respectively were used in this study. To obtain the volumetric stress under an applied load, the shear stress field was numerically integrated over the volume following a Gauss quadrature integration scheme (Foschi and Barrett 1976).

Close examination of the stress field generally reveals high stress concentrations at loading points. If these locations were considered during the evaluation of I, unrealistic estimations of longitudinal shear strength would result. Since one can assume that a combination of shear and compression perpendicular to grain type failure would occur locally. Therefore, the stresses in these regioins should be ignored during the integration. In the current analysis, the shear stresses in some of the elements located in the top rows during the evaluation of I were ignored (see Figure 8.1 to 8.6). This is consistent with the interpretation of the experimental data base where beam failures which extended into or within the 25 mm of the top and bottom zones of the beam were considered as either bending or compression perpendicular to grain failures, rather than shear failures.

Figures 11 to 14 show the compressive stresses for the nominal 38mm x 185mm and 38mm x 285mm specimens of the different species assuming the load was uniformly distributed over the loading plates. Again, loading and reaction points exhibit high compressive stress

concentration, which dissipate quickly towards the mid-depth of the beams between the loading heads and center reaction. These are the areas where almost all shear failures occurred.

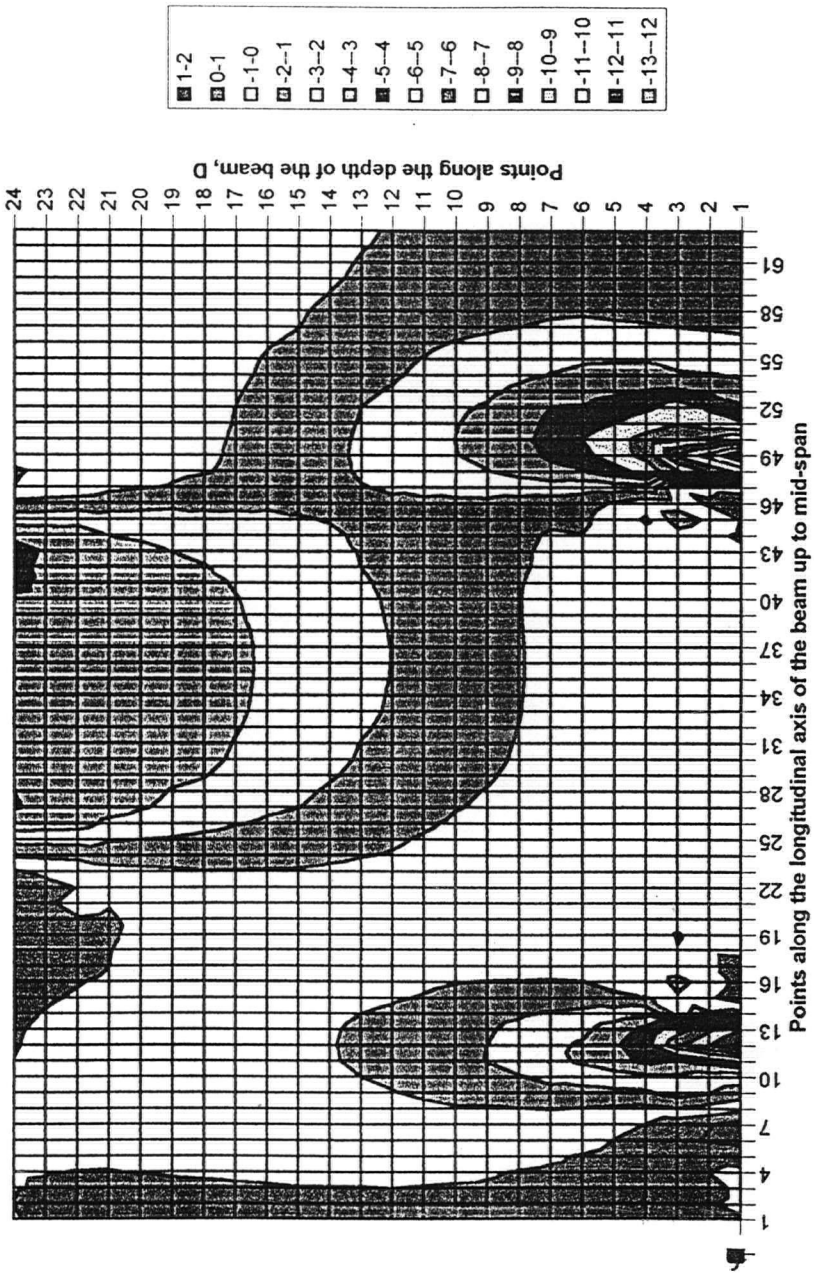


Figure 11. Compressive stresses for 38mm x 185mm 5D Spruce-Pine-Fir based on median failure load (MPa)

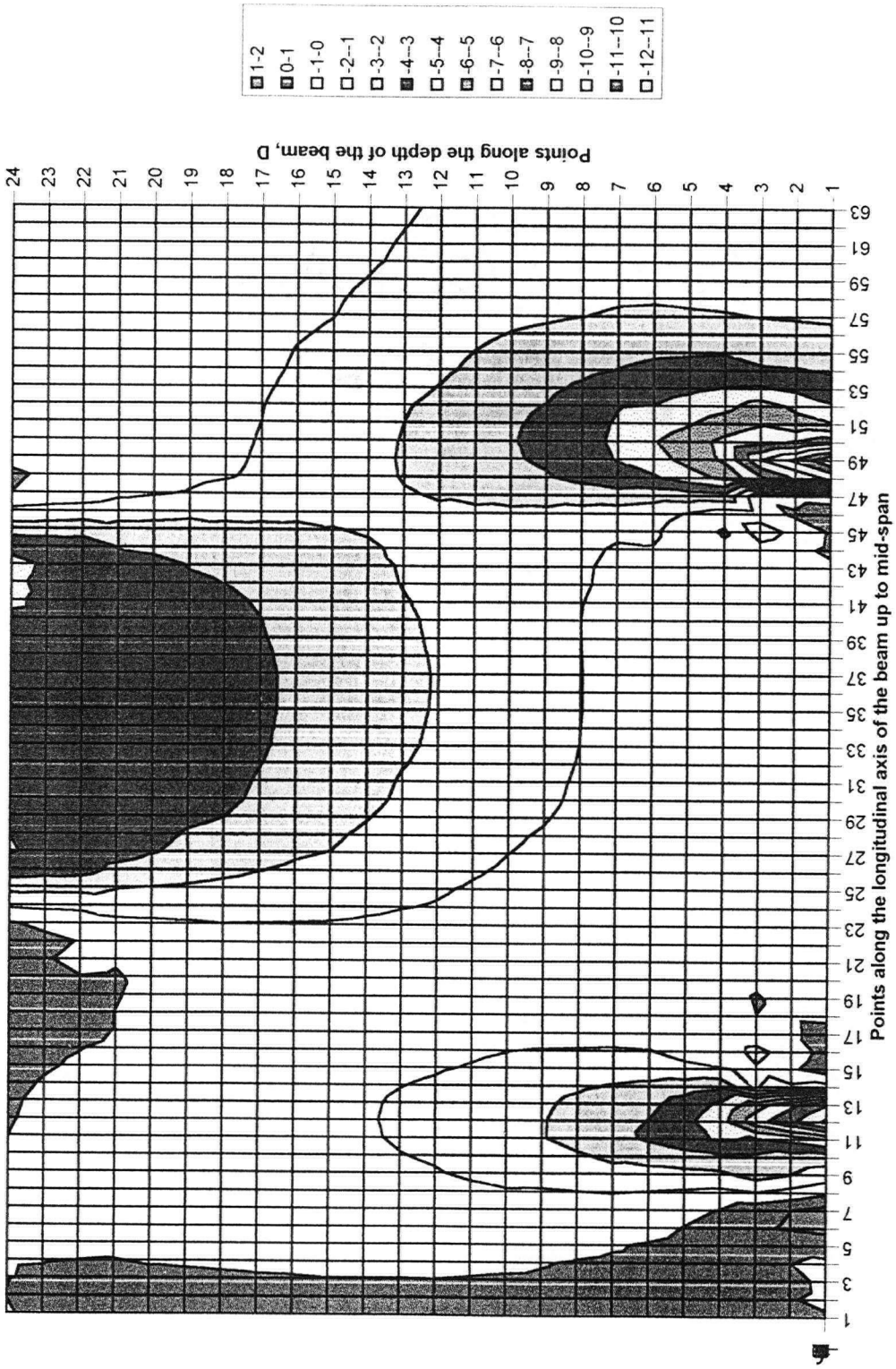


Figure 12.1. Compressive stresses for 38mm x 185mm 5D Hem-Fir based on median failure load (MPa)

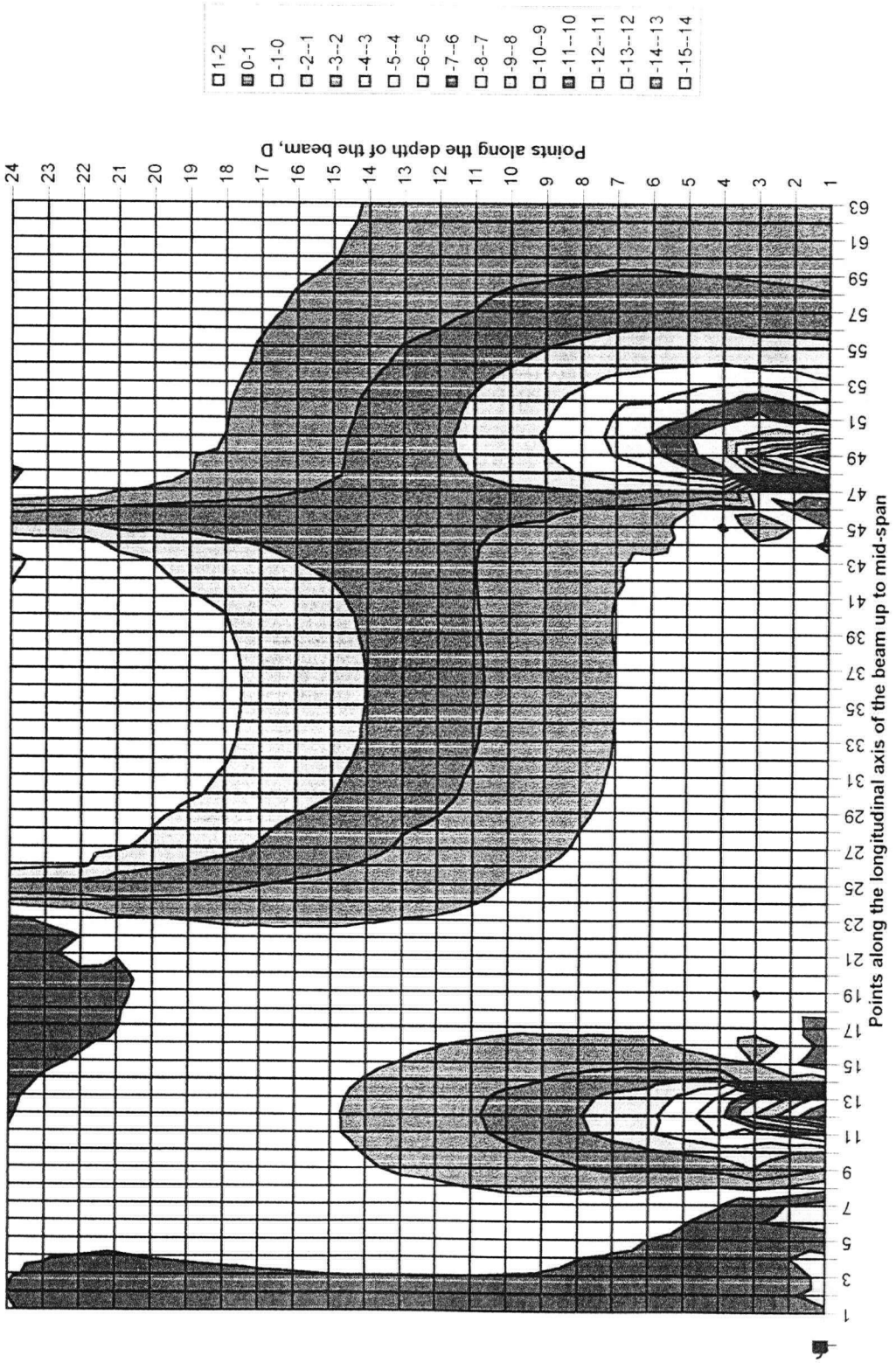


Figure 12.2 Compressive stresses for 38mm x 185mm 5D Douglas-Fir based on median failure load (MPa)

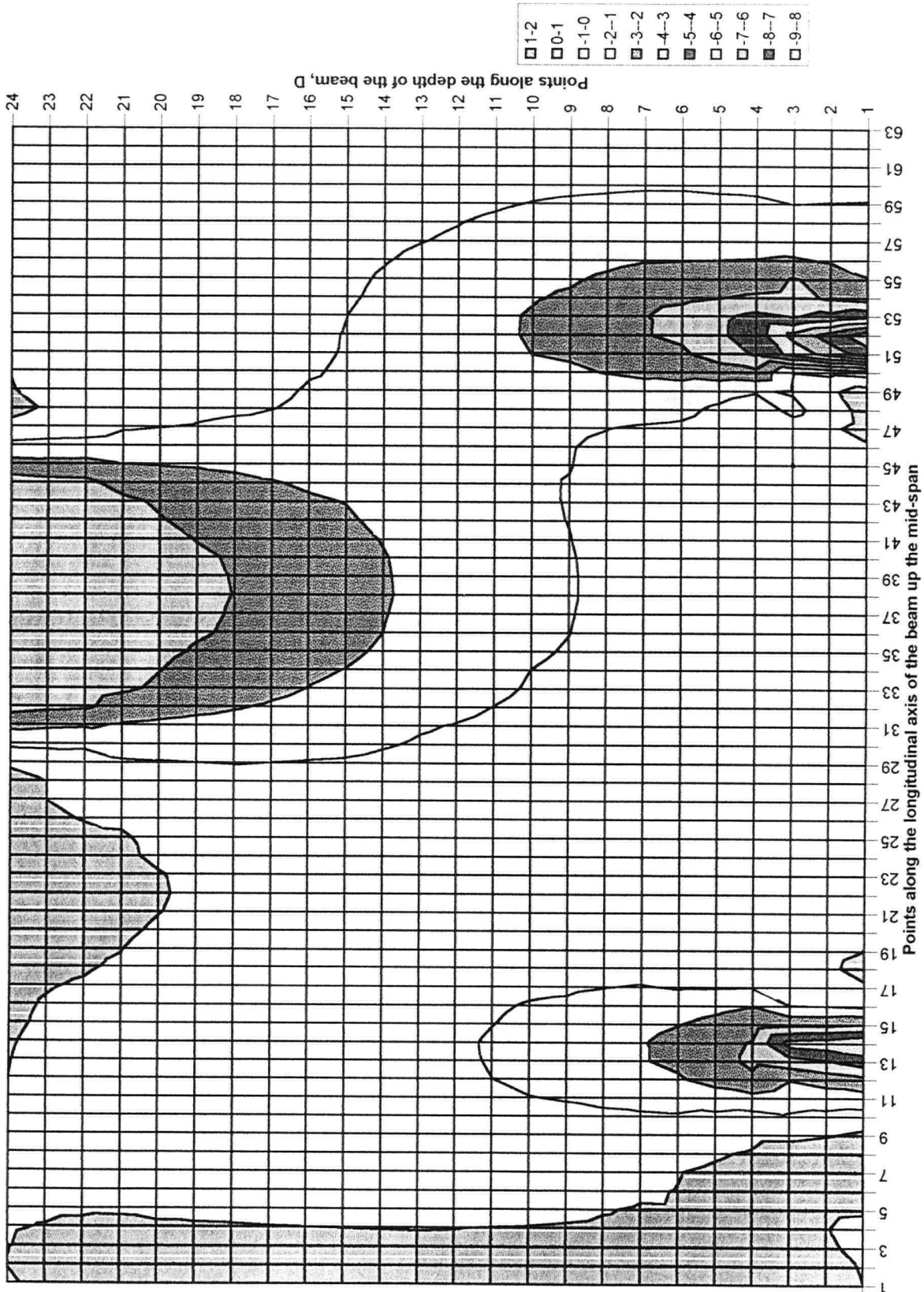


Figure 13. Compressive stresses for 38mm x 285mm 5D Spruce-Pine-Fir based on median failure load (MPa)

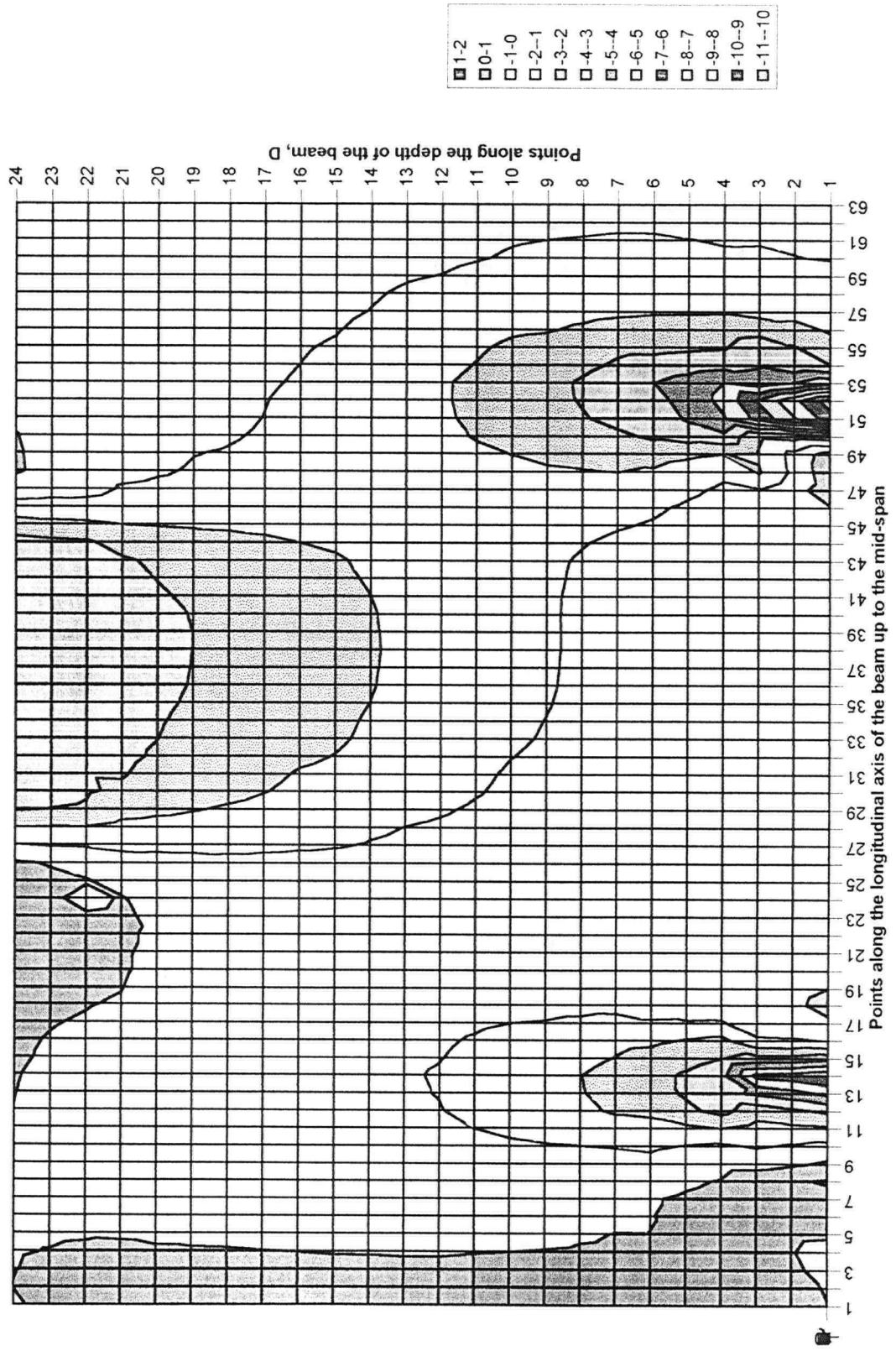


Figure 14. Compressive stresses for 38mm x 285mm 5D Hem-Fir based on median failure load (MPa)

The compressive stresses in these areas were approximately 1 to 3 MPa in the 5D cases. This would suggest that the compressive stresses in the members contribute very little, if any, to influence the shear strength.

Shown in Figures 16 to 18 are the cumulative distributions of all the failure modes except compression perpendicular to grain failures in the nominal 38mm x 185mm specimens for both 5D and 6D cases of the different species (Figures 22 and 23 for nominal 38mm x 285mm). Figures 19 to 21 are the cumulative distributions of the failure shear loads only. (Figures 24 and 25 for nominal 38mm x 285mm). From these cumulative distributions, specimens with the longer span of the same nominal size group in the 6D cases for all species exhibited lower shear strength than the shorter span 5D cases. This would suggest that size effect played a role in that the longer span cases with the larger specimen volumes had a higher probability of containing defects that lowered the shear strengths of the members.

Tables 3 to 6 compare the predictions of the finite element and Weibull weakest link analyses against the experimental median and fifth percentile beam shear strengths for both nominal sizes. The predicted median and 5th percentile failure shear loads were estimated by substituting the median and 5th percentile $\tau^*$ respectively into equation 26. The median and 5th percentile beam failure shear stresses can be estimated by equation 30 where P is the median and 5th percentile beam failure shear loads. Based on classical engineering mechanics theory and assuming point loads and simple supports, the free body, shear force, and maximum shear stress diagrams for the two span load configuration are shown in Figure 15. It is in these middle spans that almost all longitudinal shear failures occurred.

Errors between the predicted and experimental median and 5th percentile shear strength for the different nominal sizes are also provided in Tables 3 to 6. These predicted values were obtained by using equation 26 . The k values were estimated using equation 29, based on ASTM shear blocks test results of the corresponding species, independent of the failure modes and span configurations. A two parameter Weibull fit was conducted to evaluate the fifth percentile of the failure shear loads for the various species, sizes, and spans groups. The median dimensions of the members were used to calculate the failure shear stresses of equation 30.

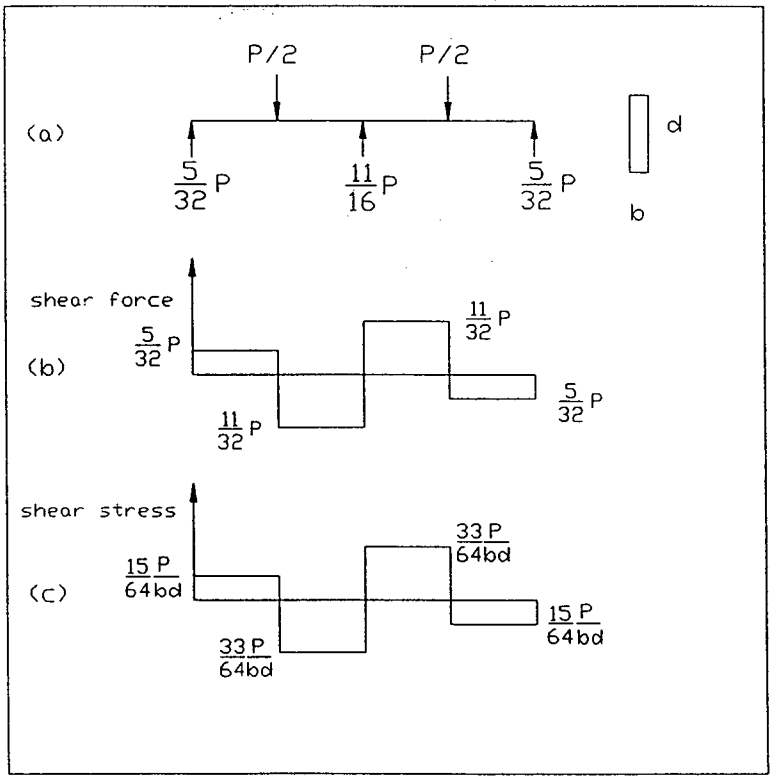


Figure 15. Classical analysis of the 5 point test system

Good agreement between the median predicted and experimental values were observed with the exception of nominal 38mm x 185mm Hem-Fir in the 6D case, which was an over-estimated by 14.96 %. This could be explained by the fact that the MOEs in this group were lower than expected, suggesting that the actual beam strength was lower than the model prediction which was based on the clear ASTM shear blocks results. Large knots were frequently encountered in this particular group. A maximum under-estimated error of -4.85% was observed for the median failure shear load.

Soltis and Rammer's (1994) proposed method to relate $\tau_{ASTM}$ to beam shear strength ($\tau$) of equation 2 did not accurately predict the failure shear loads from this study. The empirically based approach under-predicts the median failure stress with a maximum error of -4.23 % and mostly over-predicts the median failure stress with a maximum error of 31.14% Evaluating the median ASTM shear strength based on only beams that failed in shear, instead of the entire sample group regardless of the failure modes, did not improve these error statistics for the empirically based approach.

Figures 46 and 47 compares the two prediction methods with measured median failure loads from the various cases. Clearly, good agreement can be observed with the finite element and Weibull weakest link approach which tends to under-predict the median failure stress. The maximum error fluctuated between -0.86% (under-prediction) to 14.96% (over-prediction).

Contrary to the assumed k value of 5.53 for all softwood used during the development of the shear strength provision of the current Canadian Code, this study has shown that k values are

species dependent. Tables 9 and 10 compare the shear strength of a unit volume under uniform shear stress, $\tau^*$, for different species and size groups based on the current study (equation 27) and the approach taken to obtain the current Canadian Code shear strength provisions (equation 6). It is clear that using the species dependent k values of the select structural sawn lumber together with equation 27 yields a higher $\tau^*$. This would indicate that the characteristic shear strength values adopted in the current Canadian Code might be overly conservative for Select Structural dimension lumber. For lower grades of dimension lumber, shear failures typically do not govern because the bending to shear strength ratio is significantly lower as compared to the Select Structural grade material. Therefore, in lower quality dimension lumber, the bending failure mode is expected to be the most critical.

# 6. CONCLUSION

An experimental study has been conducted to evaluate the longitudinal shear strength of Canadian softwood of Select Structural grade lumber with sizes, 38mm x 185 mm and 38mm x 285mm, using a two span five point bending test procedure. Three species groups, Douglas-Fir, Hem-Fir and Spruce-Pine-Fir, have been considered. In the nominal 38mm x 185mm size group, approximately 40 % of the failures can be attributed to shear fracture compared to 30% in the nominal 38mm x 285mm size group. Two test configurations were considered: test span to specimen depth ratios of 6 and 5. ASTM shear block tests were conducted to evaluate the shear strength of small clear specimens, cut from the test beams. Based on the ASTM shear block test results, finite element analyses coupled with the Weibull weakest link theory were used to predict the shear failure loads of full size members. Good agreement between predicted and measured failure loads were observed.

During the last revision of the Canadian Code on Engineering Design in Wood, leading to CAN/CSA-086.1-M94, a reliability based approach was adopted for calculating the shear resistance of sawn lumber. These values were derived from analyses considering two distinct modes of horizontal shear failure in sawn lumber: clear wood without end splits (mode I) and with end splits (mode II). The combined probability of failure of both modes was evaluated using a uniform shear stress, $\tau^*$, that was based on an assumed species-independent Weibull parameter $k = 5.53$, derived from Douglas-Fir glued laminated beam test results.

The test results from this study show that k is species-dependent and $\tau^*$ values from sawn lumber test results are higher than those that were adopted assuming equivalency with Douglas-Fir glued laminated beam test results. This indicates that the characteristic shear strength adopted in the code might be conservative.

Further, results from this study confirmed that the load carrying capacity of sawn lumber under shear failure mode is test configuration dependent and the volumetric shear stress should be considered as the key parameter to evaluate the shear strength of beams. Two span five point bending test procedures have been proposed for the evaluation of shear strength of sawn lumber in the United States. The results from this study show that the empirically based U.S. procedures seemed to be inappropriate.

## References


ASTM. 1994a. Standard methods of testing small clear specimens of timber. ASTM D143. American Society of Testing and Materials. Philadelphia, USA

ASTM. 1994b. Establishing structural grades and related allowable properties for visually graded lumber. ASTM D245. American Society of Testing and Materials. Philadelphia, USA

Breitinger H.O., R.H. Leicester, C. Seath and P. Walsh 1994. In-grade wood beam-shear strength. In Proc. of Pacific Timber Engineering Conference. Gold Coast, Australia. July 11-15. 1:642-645.

Ethington, R. L.; Galligan, W. L.; Montery, H. M.; Freas, A. D. 1979. "Evolution of allowable stresses in shear for lumber. "Gen. Tech. Report FPL 23 Madison, WI: US Department of Agriculture. Forest Service. Forest Products Laboratory.

Foschi, R.O. and J.D. Barrett 1976. Longitudinal shear strength of Douglas-Fir. Canadian Journal of Civil Engineering. 3(2):198-208

Foschi, R.O. and J.D. Barrett 1977a. Shear strength of uniformly loaded dimension lumber. Canadian Journal of Civil Engineering. 4(1):85-96

Foschi, R.O. and J.D. Barrett 1977b. Longitudinal shear in wood beams: a design method. Canadian Journal of Civil Engineering. 4(3):363-370

Foschi, R.O., B.R. Folz, F.Z. Yao. 1989. Reliability-Based Design of Wood Structures. Structural Research Series, Report No. 34 . Department of Civil Engineering, University of British Columbia, Vancouver, Canada.

Kennedy, E. 1965. Strength and related properties of woods grown in Canada. Dept. of Forestry Pub. No. 1104, pp. 24-25.

Leicester, R.H. and H.O. Breitinger. 1991. A Discrete co-relationship with Weibull. 1991 International Timber Engineering Conference, London.

Leicester, R.H. and H.O. Breitinger. 1992. Measurement of beam shear strength. In Proc. of IUFRO S.05.02 Timber Engineering Meeting. Bordeaux, France. August 17-21. 12pp.

Liu, J.Y. 1980. Shear strength of wood beams: a Weibull analysis. Journal of structural division. ASCE. 106(10):2035-2052.

Soltis, L.A. and DR Rammer. 1994. Shear strength of unchecked glued laminated beams. Forest Products Journal. 44(1):51-57

Weibull, W. 1939. A statistical theory of strength of materials. Swedish Royal Institute of Engineering Research. Report No. 151. Stockholm, Sweden.

# APPENDIX A

Table 1. Summary statistical results for the nondestructive testing for 38 mm x 185 mm specimens.

| | Edgewise modulus of elasticity | | | | Flat-wise modulus of elasticity | | | Oven Dry Specific Gravity | |
|---|---|---|---|---|---|---|---|---|---|
| 38mmx185mm | Sample size | Median (MPa) | Mean (MPa) | CV (%) | Median (MPa) | Mean (MPa) | CV (%) | Median | CV (%) |
| Entire Sample | | | | | | | | | |
| Douglas-Fir | 102 | 12300 | 12802 | 29.42 | 12451 | 12346 | 14.21 | 0.492 | 9.78 |
| Hem-Fir | 102 | 9611 | 10227 | 29.30 | 9668 | 9747 | 13.26 | 0.449 | 8.79 |
| Spruce-Pine-Fir | 94 | 10991 | 11538 | 23.21 | 10923 | 10811 | 12.51 | 0.412 | 11.31 |
| 5D | | | | | | | | | |
| Douglas-Fir | 48 | 11522 | 12296 | 29.91 | 12144 | 12152 | 15.44 | 0.496 | 10.03 |
| Hem-Fir | 42 | 10567 | 10879 | 25.10 | 9472 | 9490 | 13.52 | 0.449 | 6.78 |
| Spruce-Pine-Fir | 51 | 10707 | 11281 | 21.25 | 10652 | 10840 | 12.88 | 0.399 | 12.07 |
| 6D | | | | | | | | | |
| Douglas-Fir | 54 | 12799 | 13252 | 28.80 | 12671 | 12519 | 13.09 | 0.486 | 9.65 |
| Hem-Fir | 60 | 8858 | 9771 | 31.80 | 9854 | 9927 | 12.88 | 0.449 | 10.01 |
| Spruce-Pine-Fir | 43 | 11286 | 11841 | 25.14 | 11115 | 10777 | 12.20 | 0.419 | 10.26 |

Table 2. Summary statistical results for the nondestructive testing for 38 mm x 285 mm specimens.

| | Edgewise modulus of elasticity | | | | Flat-wise modulus of elasticity | | | Oven Dry Specific Gravity | |
|---|---|---|---|---|---|---|---|---|---|
| 38mmx285mm | Sample size | Median (MPa) | Mean (MPa) | CV (%) | Median (MPa) | Mean (MPa) | CV (%) | Median | CV (%) |
| Entire Sample | | | | | | | | | |
| Hem-Fir | 101 | 10707 | 10593 | 17.47 | 10171 | 10094 | 11.32 | 0.426 | 8.61 |
| Spruce-Pine-Fir | 103 | 10199 | 10259 | 14.09 | 9643 | 9529 | 10.97 | 0.372 | 10.65 |
| 5D | | | | | | | | | |
| Hem-Fir | 48 | 10144 | 10402 | 20.22 | 1287 | 9999 | 12.87 | 0.432 | 6.69 |
| Spruce-Pine-Fir | 52 | 10033 | 10348 | 15.60 | 9642 | 9472 | 12.62 | 0.369 | 10.99 |
| 6D | | | | | | | | | |
| Hem-Fir | 53 | 10813 | 10767 | 14.76 | 10190 | 10188 | 9.80 | 0.419 | 10.11 |
| Spruce-Pine-Fir | 51 | 10296 | 10169 | 12.38 | 9650 | 9588 | 9.10 | 0.376 | 10.39 |

Table 3. Predicted and experimental median results for 38 mm x 185 mm specimens.

| 38mm x 185mm | Experimental Results | | | | Model Predictions | | | | |
|---|---|---|---|---|---|---|---|---|---|
| | | | | | FE and Weibull analysis | | | Soltis and Rammer | |
| | Median Failure Load (kN) | Median Failure Stress (MPa) | CV (%) | No. of shear/ sample size | Median Failure Load (kN) | Median Failure Stress (MPa) | Error (%) | Median Failure Stress (MPa) | Error (%) |
| (5D) | | | | | | | | | |
| Douglas-Fir | 134.80 | 9.46 | 14.04 | 25/48 | 132.79 | 9.32 | -1.52 | 9.06 | -4.23 |
| Hem-Fir | 111.70 | 7.86 | 16.12 | 25/42 | 115.22 | 8.11 | 3.06 | 8.35 | 6.16 |
| Spruce-Pine-Fir | 109.15 | 7.74 | 15.51 | 14/51 | 104.10 | 7.38 | -4.85 | 7.73 | -0.14 |
| (6D) | | | | | | | | | |
| Douglas-Fir | 122.66 | 8.60 | 12.54 | 28/54 | 118.77 | 8.33 | -3.27 | 8.73 | 1.47 |
| Hem-Fir | 88.50 | 6.23 | 19.05 | 26/60 | 104.07 | 7.32 | 14.96 | 8.05 | 29.19 |
| Spruce-Pine-Fir | 95.30 | 6.76 | 9.61 | 12/43 | 93.35 | 6.62 | -2.09 | 7.45 | 10.28 |
| | Based on sheared beam specimens only | | | | | | | | |
| (5D) | | | | | | | | | |
| Douglas-Fir | 134.80 | 9.46 | 14.04 | 25/48 | | | | 9.287 | -1.78 |
| Hem-Fir | 111.70 | 7.86 | 16.12 | 25/42 | | | | 8.567 | 8.984 |
| Spruce-Pine-Fir | 109.15 | 7.74 | 15.51 | 14/51 | | | | 8.166 | 5.479 |
| (6D) | | | | | | | | | |
| Douglas-Fir | 122.66 | 8.60 | 12.54 | 28/54 | | | | 8.955 | 4.073 |
| Hem-Fir | 88.50 | 6.23 | 19.05 | 26/60 | | | | 8.26 | 32.628 |
| Spruce-Pine-Fir | 95.30 | 6.76 | 9.61 | 12/43 | | | | 7.873 | 16.48 |

Table 4. Predicted and experimental results for 38 mm x 285 mm specimens.

| 38mm x 285mm | Experimental Results | | | | Model Predictions | | | | |
|---|---|---|---|---|---|---|---|---|---|
| | | | | | FE and Weibull analysis | | | Soltis and Rammer | |
| | Median Failure Load (kN) | Median Failure Stress (MPa) | CV (%) | No. of shear/ sample size | Median Failure Load (kN) | Median Failure Stress (MPa) | Error (%) | Median Failure Stress (MPa) | Error (%) |
| (5D) | | | | | | | | | |
| Hem-Fir | 138 | 6.6 | 9.97 | 19/48 | 133.7 | 6.38 | -3.2 | 7.23 | 9.72 |
| Spruce-Pine-Fir | 115.9 | 5.5 | 11.1 | 12/52 | 117.6 | 5.58 | 1.44 | 6.47 | 17.59 |
| (6D) | | | | | | | | | |
| Hem-Fir | 115.1 | 5.5 | 8.9 | 17/53 | 108.64 | 5.18 | -5.94 | 6.97 | 26.83 |
| Spruce-Pine-Fir | 100.2 | 4.76 | 9.8 | 10/51 | 99.33 | 4.72 | -0.86 | 6.24 | 31.14 |
| | Based on sheared beam specimens only | | | | | | | | |
| (5D) | | | | | | | | | |
| Hem-Fir | 138 | 6.6 | 9.97 | 19/48 | | | | 7.152 | 8.54 |
| Spruce-Pine-Fir | 115.9 | 5.5 | 11.1 | 12/52 | | | | 7.16 | 30.08 |
| (6D) | | | | | | | | | |
| Hem-Fir | 115.1 | 5.5 | 8.9 | 17/53 | | | | 6.896 | 25.48 |
| Spruce-Pine-Fir | 100.2 | 4.76 | 9.8 | 10/51 | | | | 6.907 | 45.07 |

Table 5. 5th percentile predicted and experimental results for 38 mm x 185 mm specimens.

| 38mm x 185mm | Experimental Results | | Model Predictions | | | | |
|---|---|---|---|---|---|---|---|
| | | | FE and Weibull analysis | | | Soltis and Rammer | |
| | 5th percentile Failure Load (kN) | 5th percentile Failure Stress (MPa) | 5th percentile Failure Load (kN) | 5th percentile Failure Stress (MPa) | Error (%) | 5th percentile Failure Stress (MPa) | Error (%) |
| (5D) | | | | | | | |
| Douglas-Fir | 96.73 | 6.79 | 93.48 | 6.56 | -3.47 | 6.38 | -6.04 |
| Hem-Fir | 75.39 | 5.31 | 83.70 | 5.89 | 9.93 | 6.06 | 14.25 |
| Spruce-Pine-Fir | 75.70 | 5.36 | 72.51 | 5.14 | -4.40 | 5.39 | 0.30 |
| (6D) | | | | | | | |
| Douglas-Fir | 90.66 | 6.36 | 83.62 | 5.87 | -8.42 | 6.15 | -3.35 |
| Hem-Fir | 55.60 | 3.91 | 75.60 | 5.32 | 26.44 | 5.84 | 49.37 |
| Spruce-Pine-Fir | 73.48 | 5.21 | 65.03 | 4.61 | -13.00 | 5.19 | -0.37 |

Table 6. 5th percentile predicted and experimental results for 38 mm x 285 mm specimens.

| 38mm x 285mm | Experimental Results | | Model Predictions | | | | |
|---|---|---|---|---|---|---|---|
| | | | FE and Weibull analysis | | | Soltis and Rammer | |
| | 5th percentile Failure Load (kN) | 5th percentile Failure Stress (MPa) | 5th percentile Failure Load (kN) | 5th percentile Failure Stress (MPa) | Error (%) | 5th percentile Failure Stress (MPa) | Error (%) |
| (5D) | | | | | | | |
| Hem-Fir | 109.75 | 5.24 | 98.05 | 4.68 | -11.93 | 5.3 | 1.17 |
| Spruce-Pine-Fir | 90.81 | 4.32 | 82.81 | 3.93 | -9.66 | 4.56 | 5.68 |
| (6D) | | | | | | | |
| Hem-Fir | 94.41 | 4.5 | 79.67 | 3.8 | -18.46 | 5.11 | 13.4 |
| Spruce-Pine-Fir | 76.74 | 3.65 | 69.95 | 3.32 | -9.71 | 4.4 | 20.58 |

Table 7. Elasticity values used in the finite element analyses for 38 mm x 185 mm specimens.

| 38mm x 185mm | Modulus of Elasticity x-direction (MPa) | Modulus of Elasticity y-direction (MPa) | Modulus of Rigidity (MPa) | Poisson Ratios $v_{xy}$ | Poisson Ratios $v_{yx}$ |
|---|---|---|---|---|---|
| Douglas-Fir | 12300 | 595 | 757 | 0.42 | 0.03 |
| Hem-Fir | 9611 | 504 | 715 | 0.42 | 0.03 |
| Spruce-Pine-Fir | 10991 | 552 | 738 | 0.42 | 0.03 |

Table 8. Elasticity values used in the finite element analyses for 38 mm x 285 mm specimens.

| 38mm x 285mm | Modulus of Elasticity x-direction (MPa) | Modulus of Elasticity y-direction (MPa) | Modulus of Rigidity (MPa) | Poisson Ratios $v_{xy}$ | Poisson Ratios $v_{yx}$ |
|---|---|---|---|---|---|
| Hem-Fir | 10707 | 542 | 733 | 0.42 | 0.03 |
| Spruce-Pine-Fir | 10199 | 525 | 725 | 0.42 | 0.03 |

Table 9. Clear wood shear strength parameters for 38 mm x 185 mm specimens.

| | $\tau_{ASTM}$ | | | | | [4]Shear strength of a unit volume (inch^3) | | [5]Shear strength of a unit volume (inch^3) | | |
|---|---|---|---|---|---|---|---|---|---|---|
| | | | | | | median | 5th percentile | | mean | 5th percentile |
| | Median | CV | 5th percentile | Sample | k | $\tau$*0.5 | $\tau$*0.05 | assumed | $\tau$*0.5 | $\tau$*0.05 |
| 38 mm x 185 mm | (MPa) | (%) | (MPa) | size | | (MPa) | (MPa) | $\kappa$ | (MPa) | (MPa) |
| Douglas-Fir | 8.98 | 15.89 | 6.32 | 102 | 7.36 | 22.61 | 15.91 | 5.53 | 12.04 | 6.25 |
| Hem-Fir | 8.27 | 16.00 | 6.00 | 102 | 7.42 | 20.94 | 15.21 | 5.53 | 9.32 | 4.48 |
| Spruce-Pine Fir | 7.65 | 16.00 | 5.33 | 93 | 6.95 | 18.47 | 12.87 | 5.53 | 8.74 | 4.10 |
| | $\tau_{ASTM}$ results corresponding to those beams that failed in shear only. | | | | | | | | | |
| Douglas-Fir | 9.21 | 17.28 | | 53 | | | | | | |
| Hem-Fir | 8.49 | 11.59 | | 51 | | | | | | |
| Spruce-Pine Fir | 8.08 | 19.17 | | 26 | | | | | | |

Table 10. Clear wood shear strength parameters for 38 mm x 285 mm specimens.

| | $\tau_{ASTM}$ | | | | | [4]Shear strength of a unit volume (inch^3) | | [5]Shear strength of a unit volume (inch^3) | | |
|---|---|---|---|---|---|---|---|---|---|---|
| | | | | | | median | 5th percentile | | mean | 5th percentile |
| | Median | CV | 5th percentile | Sample | k | $\tau$*0.5 | $\tau$*0.05 | assumed | $\tau$*0.5 | $\tau$*0.05 |
| 38 mm x 285 mm | (MPa) | (%) | (MPa) | size | | (MPa) | (MPa) | $\kappa$ | (MPa) | (MPa) |
| Hem-Fir | 7.74 | 14.51 | 6.00 | 101 | 7.42 | 19.61 | 14.38 | 5.53 | 9.32 | 4.48 |
| Spruce-Pine Fir | 6.94 | 16.08 | 5.32 | 103 | 6.95 | 16.76 | 11.80 | 5.53 | 8.74 | 4.10 |
| | $\tau_{ASTM}$ results corresponding to those beams that failed in shear only. | | | | | | | | | |
| Hem-Fir | 7.66 | 12.07 | | 36 | | | | | | |
| Spruce-Pine Fir | 7.68 | 13.56 | | 22 | | | | | | |

[4] $\tau$* evaluated by finite element approach of equation 27

[5] $\tau$* evaluated by assumed k and $\lambda$= 1.95 of equation 6 (Foschi,Folz,Yao 1989)

# APPENDIX B

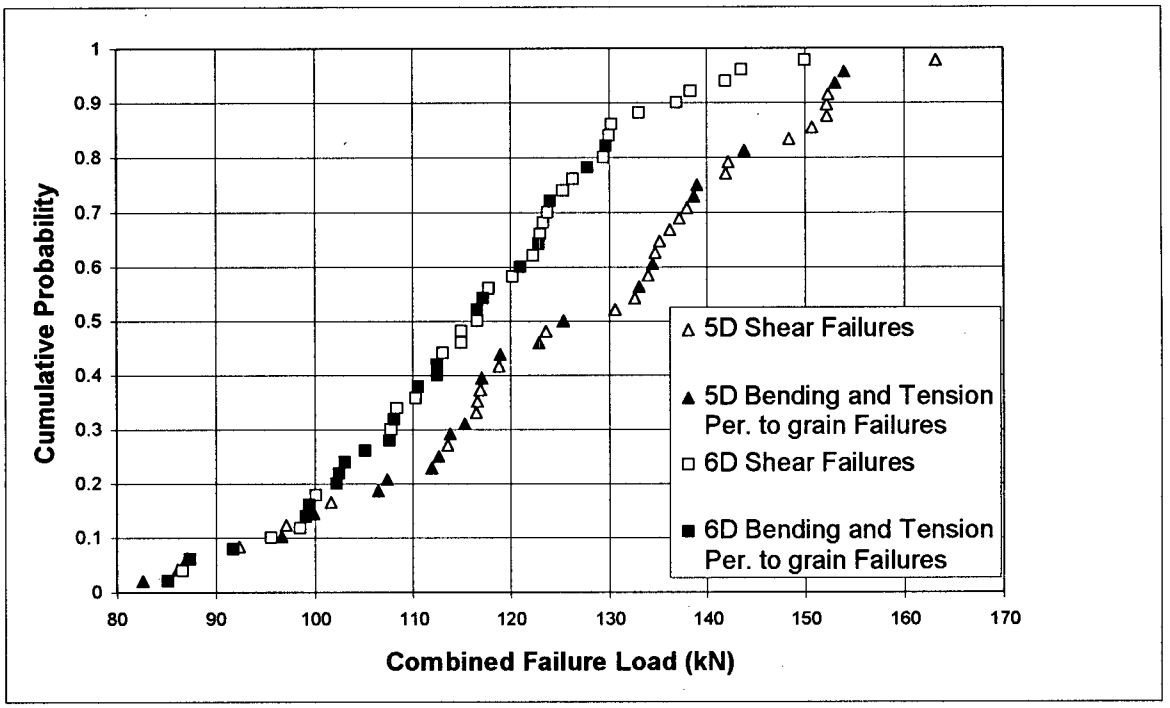


Figure 16. Cumulative probability distributions of failure loads for Douglas-Fir ( 38 mm x 185 mm)

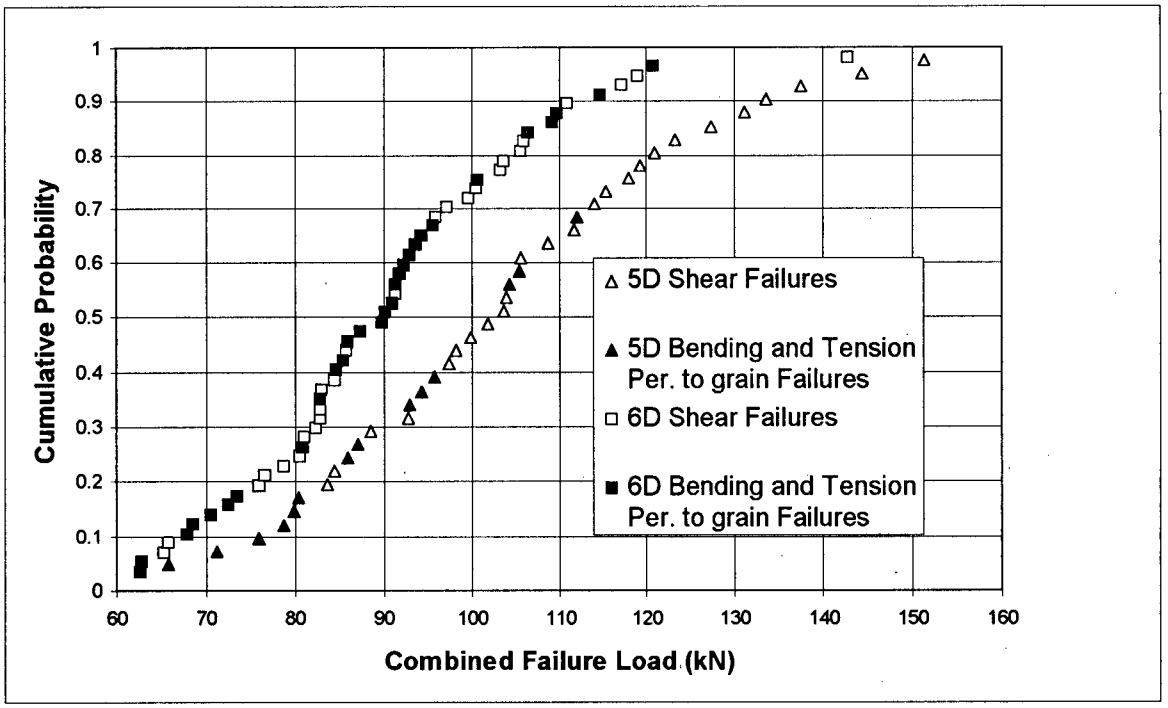


Figure 17. Cumulative probability distributions of failure loads for Hem-Fir ( 38 mm x 185 mm)

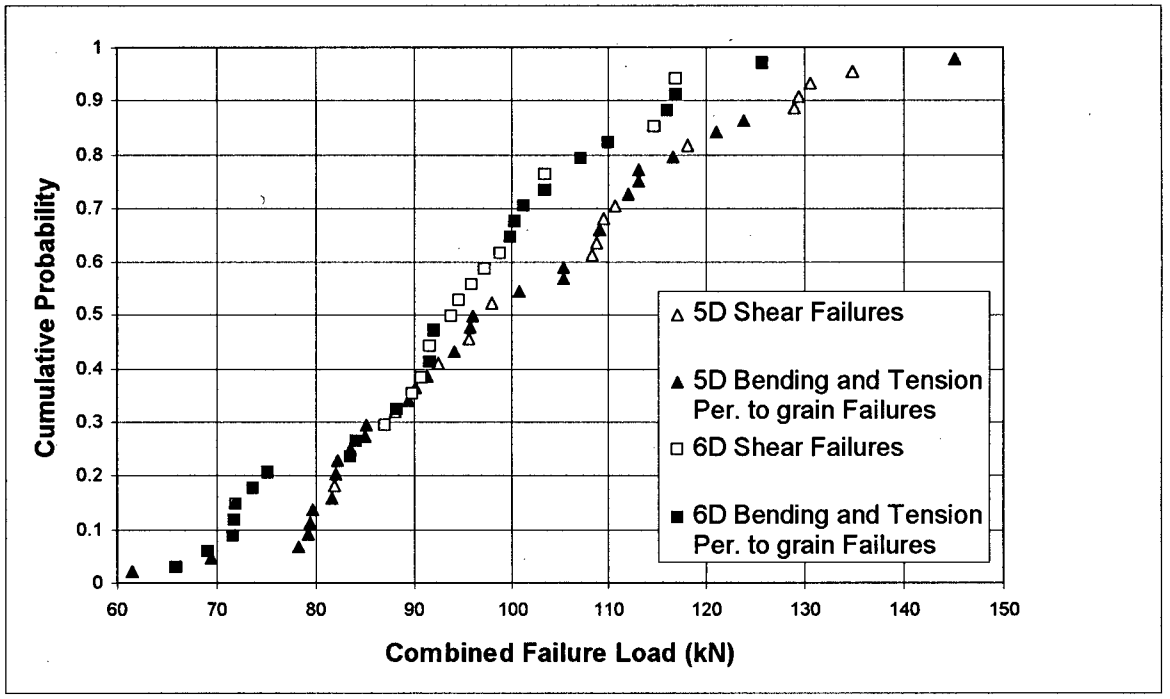


Figure 18. Cumulative probability distributions of failure loads for Spruce-Pine-Fir ( 38 mm x 185 mm)

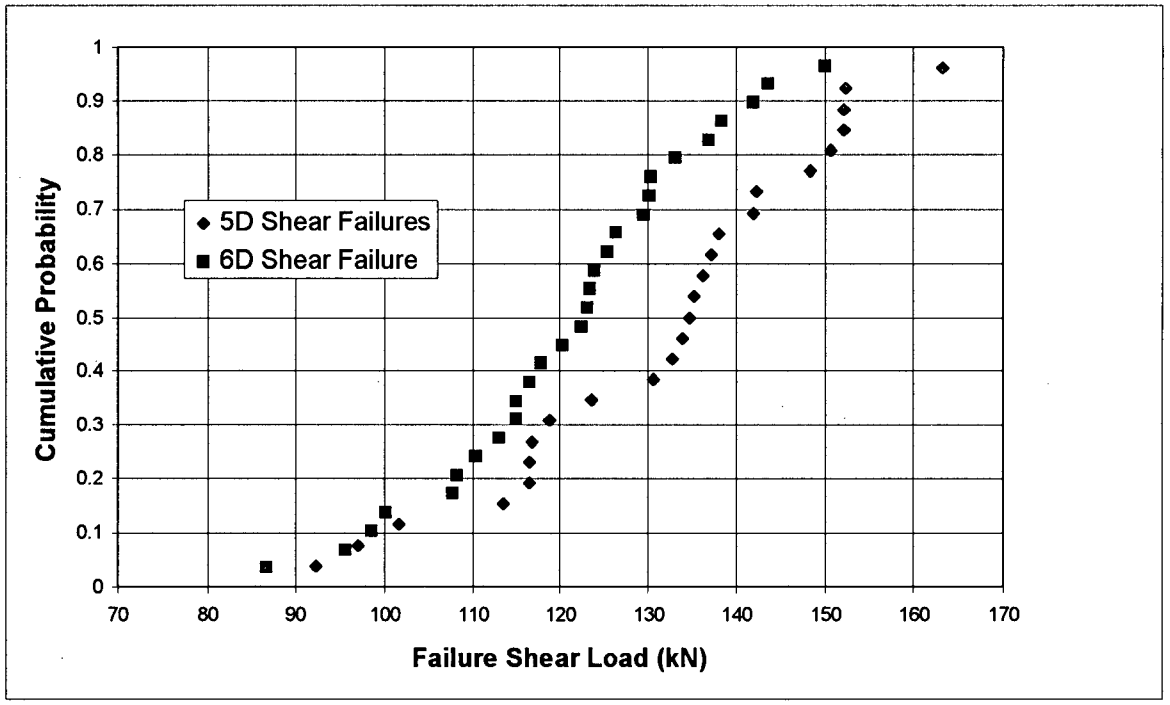


Figure 19. Cumulative probability distributions of failure loads in shear for Douglas-Fir (38 mm x 185 mm)

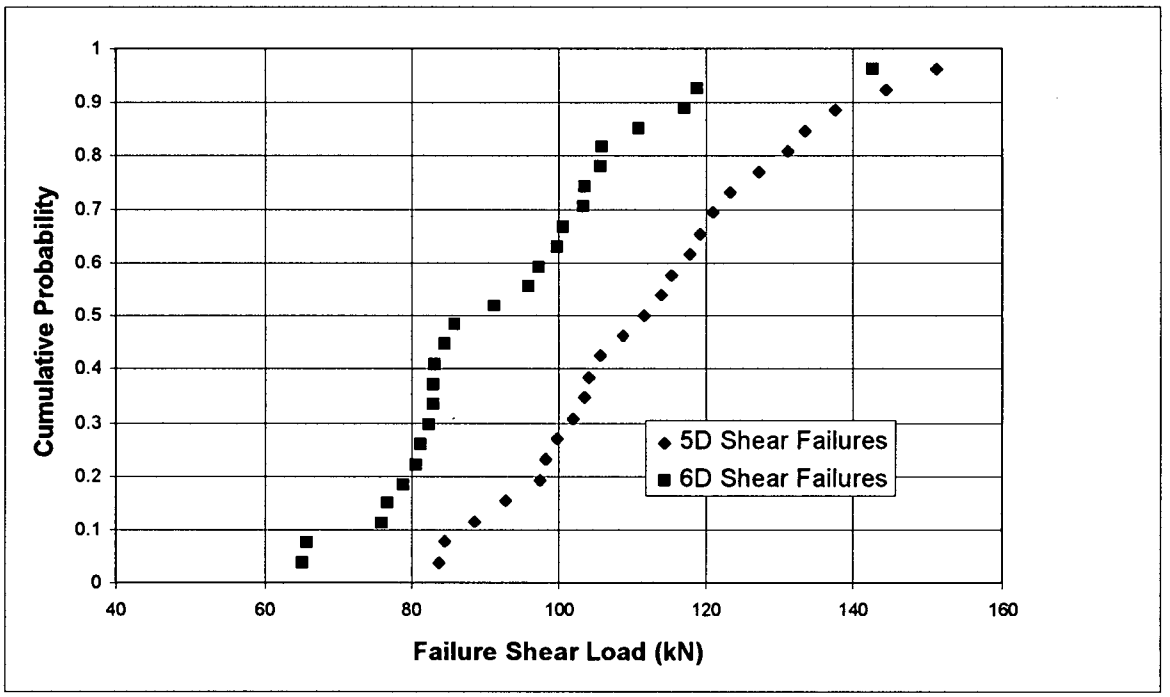


Figure 20. Cumulative probability distributions of failure loads in shear for Hem-Fir ( 38 mm x 185 mm)

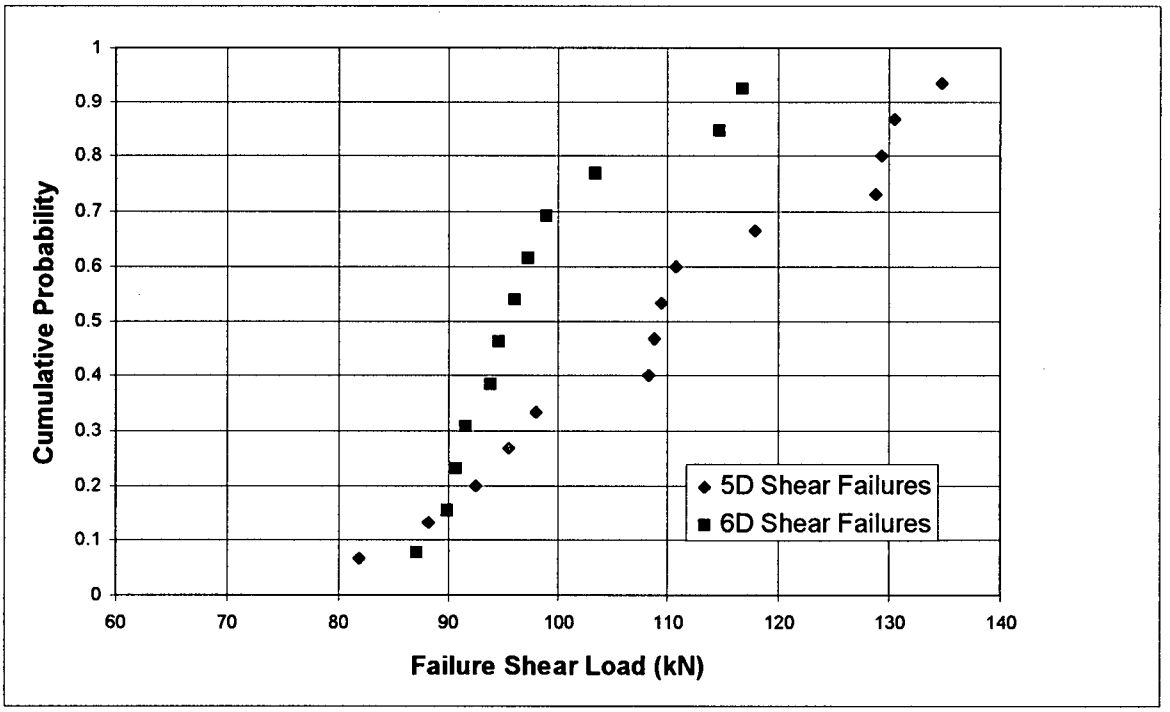


Figure 21. Cumulative probability distributions of failure loads in shear for Spruce-Pine-Fir ( 38 mm x 185 mm)

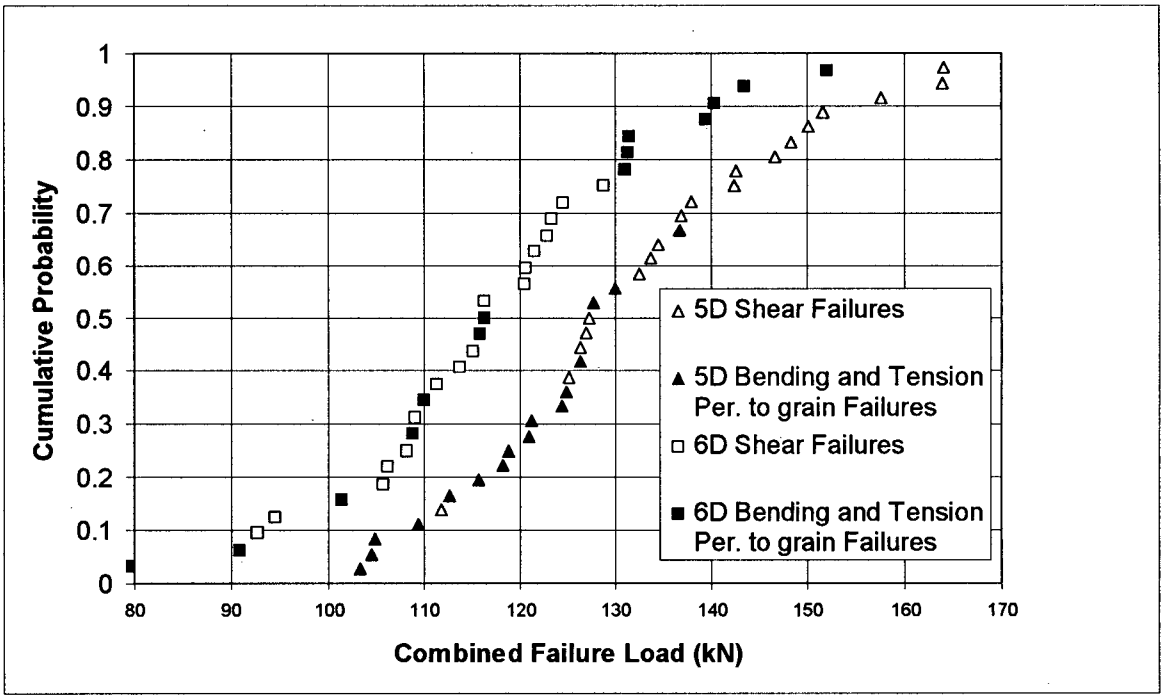


Figure 22. Cumulative probability distributions of Failure loads for Hem-Fir. ( 38 mm x 285 mm)

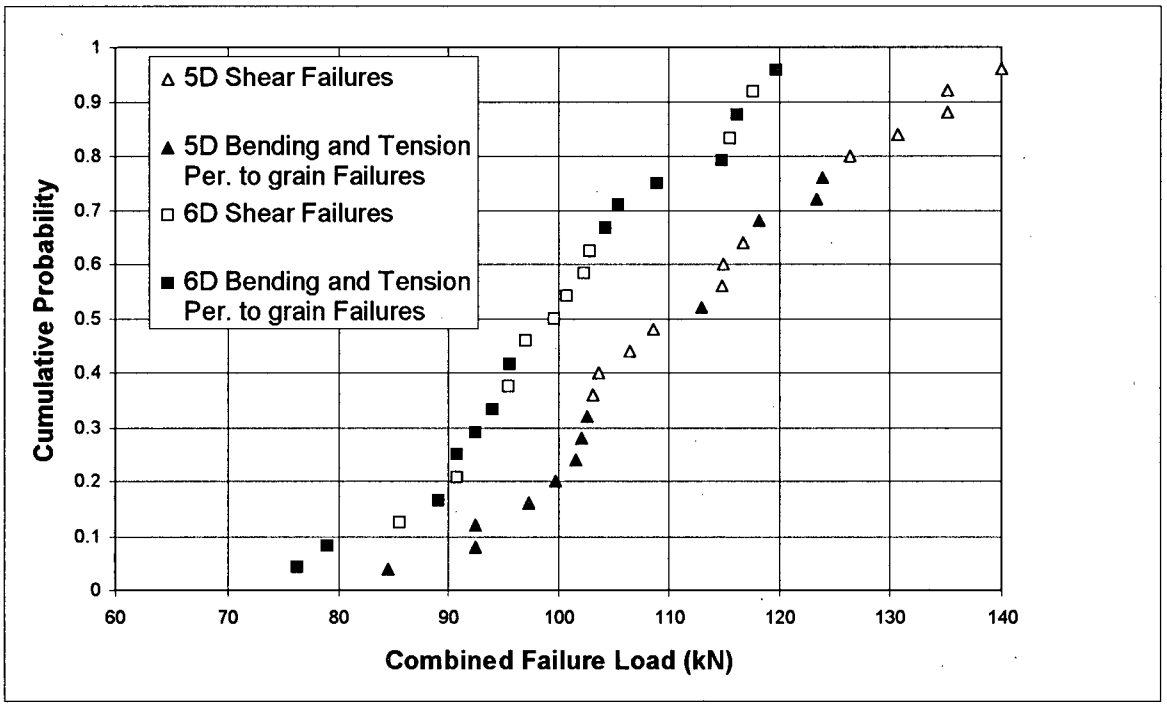


Figure 23. Cumulative probability distributions of Failure loads for Spruce-Pine-Fir. ( 38 mm x 285 mm)

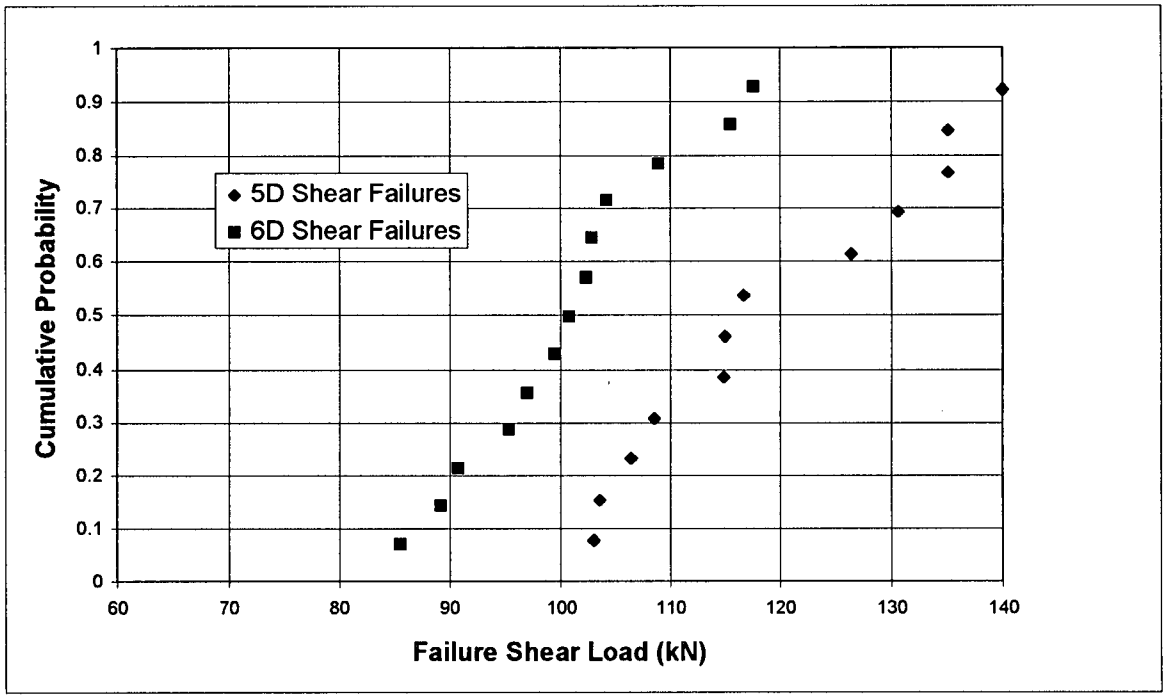


Figure 24. Cumulative probability distributions of Failure loads in shear for Hem-Fir ( 38 mm x 285 mm).

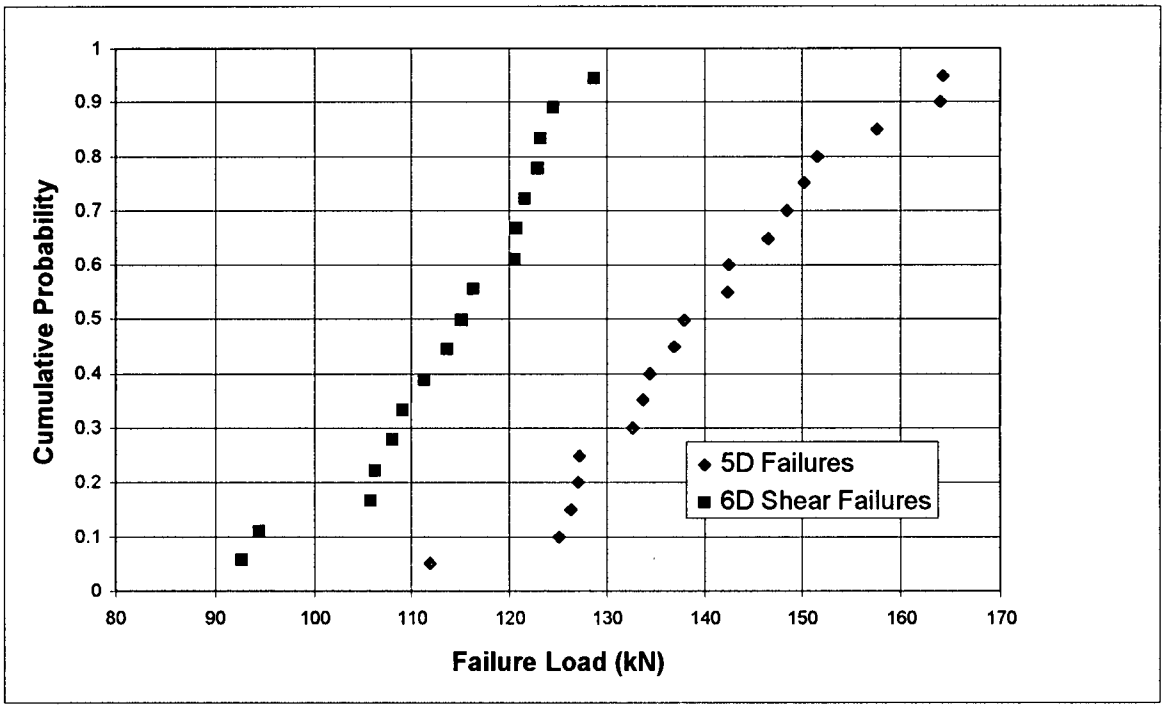


Figure 25. Cumulative probability distributions of Failure loads in shear for Spruce-Pine-Fir ( 38 mm x 285 mm).

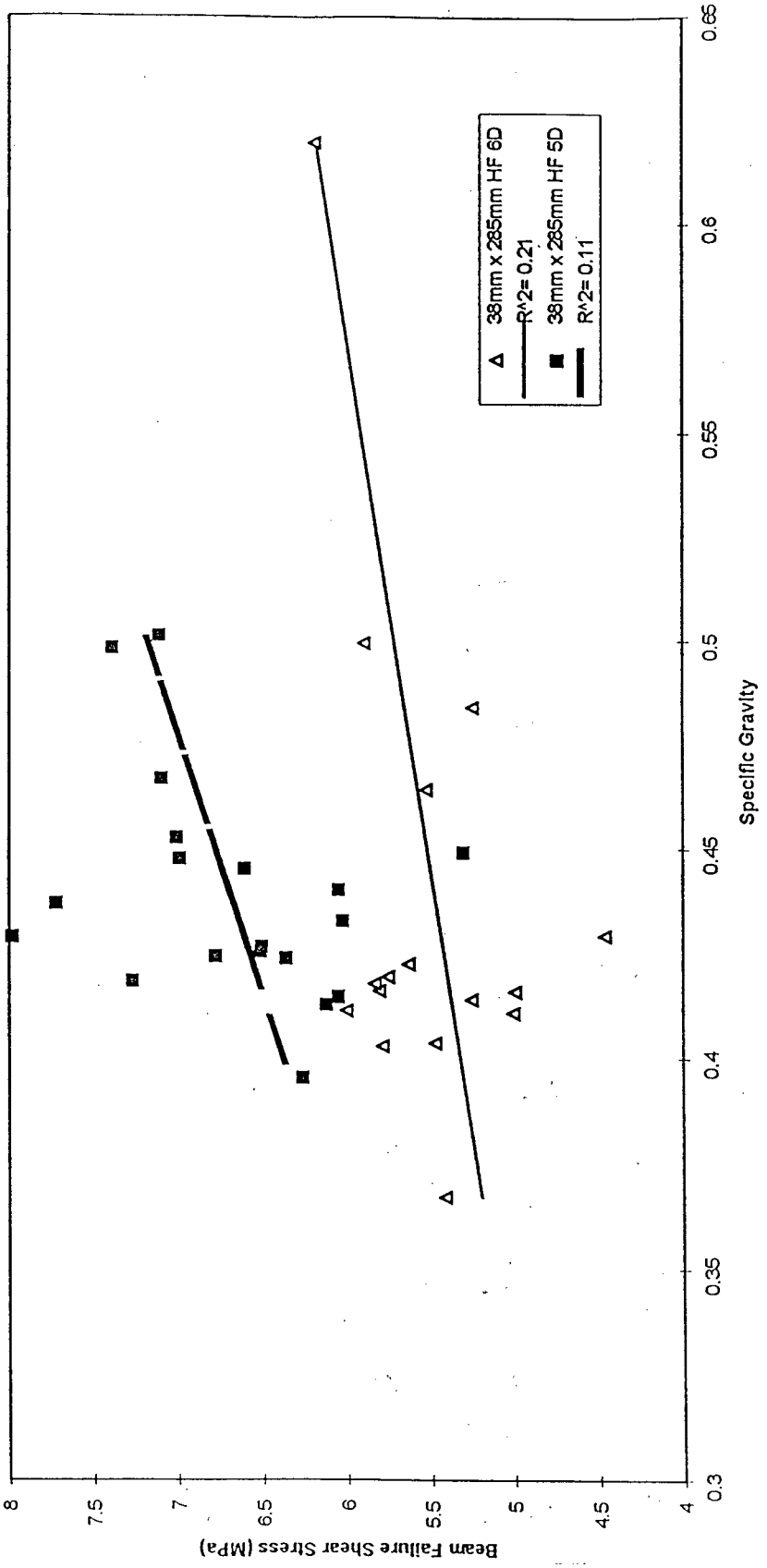


Figure 26 38mmx285mm Hem-Fir failure shear stress vs. oven dry specific gravity

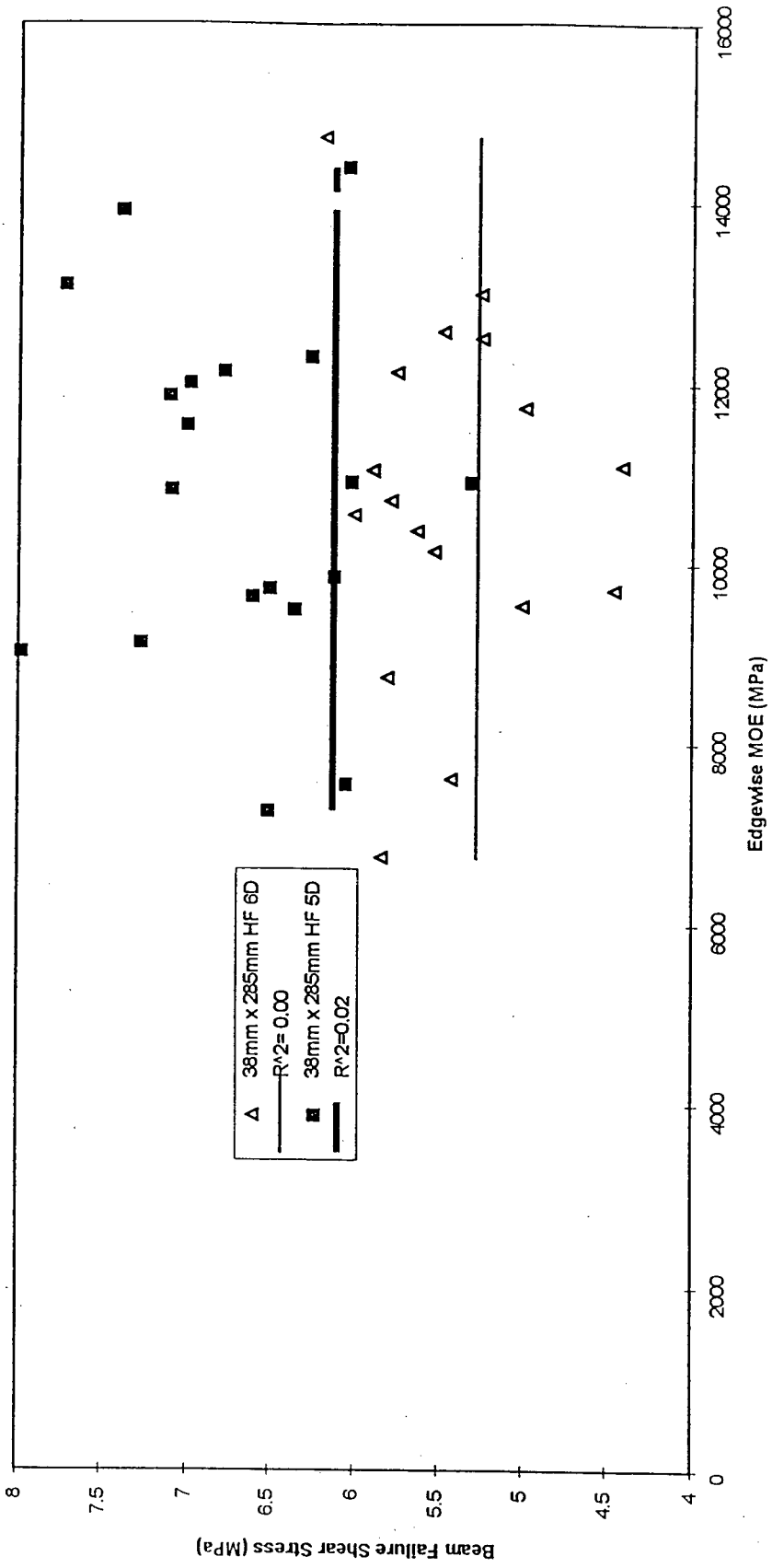


Figure 27 38mmx285mm Hem-Fir failure shear stress vs. edge-wise MOE

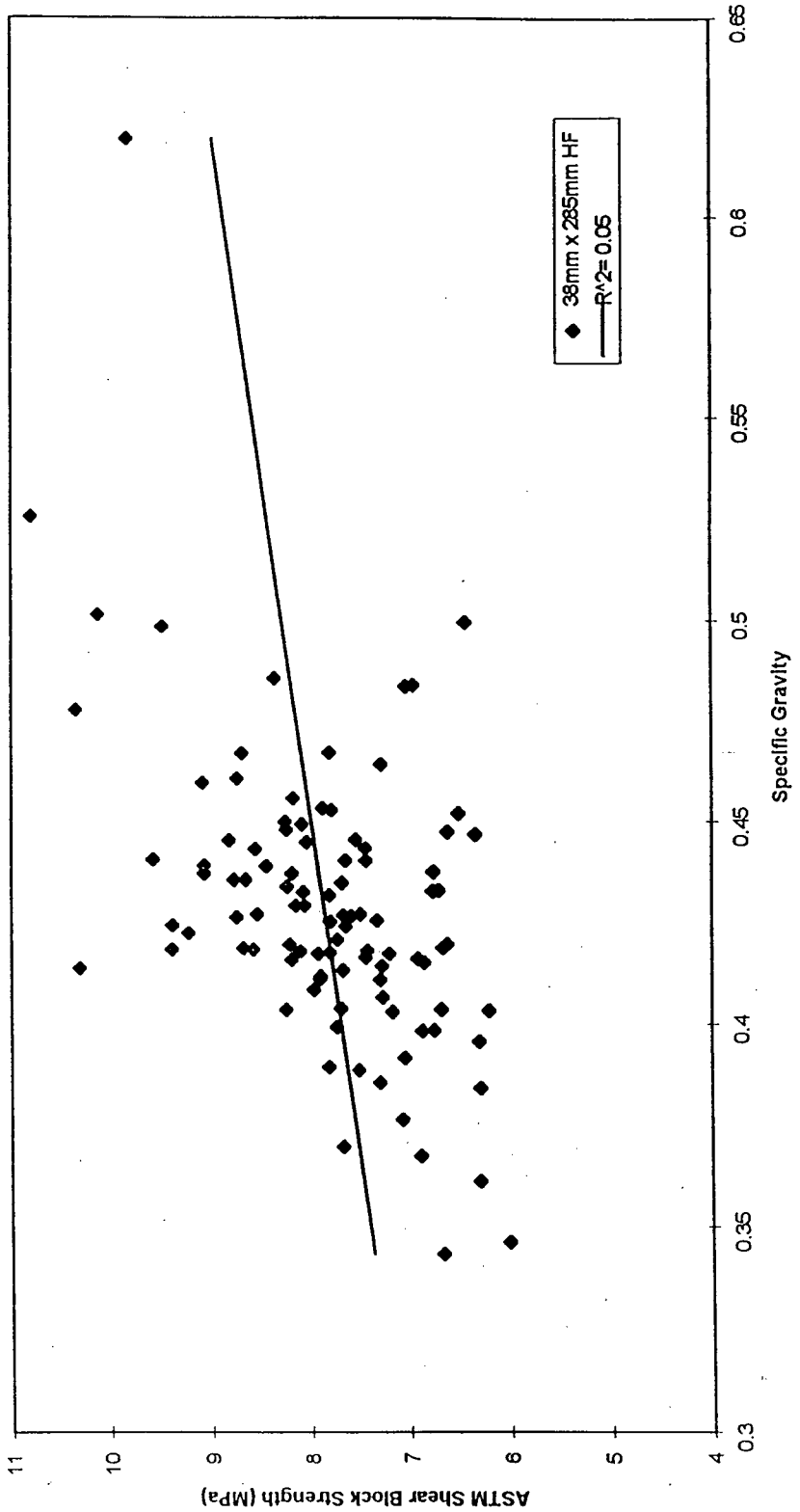


Figure 28 38mmx285mm Hem-Fir ASTM shear block strength vs. oven dry specific gravity

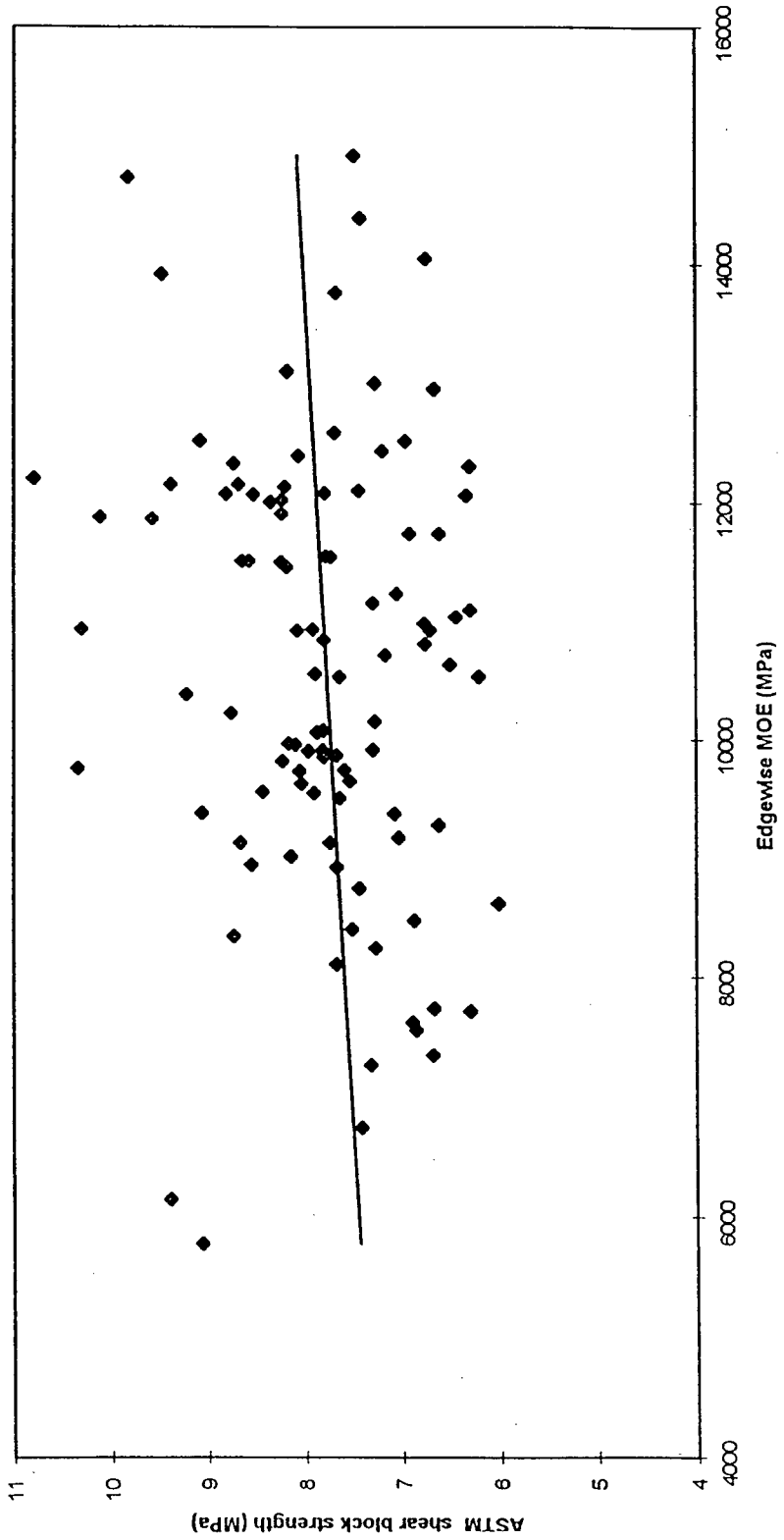


Figure 29 38mmx285mm Hem-Fir ASTM shear block strength vs. edgewise MOE

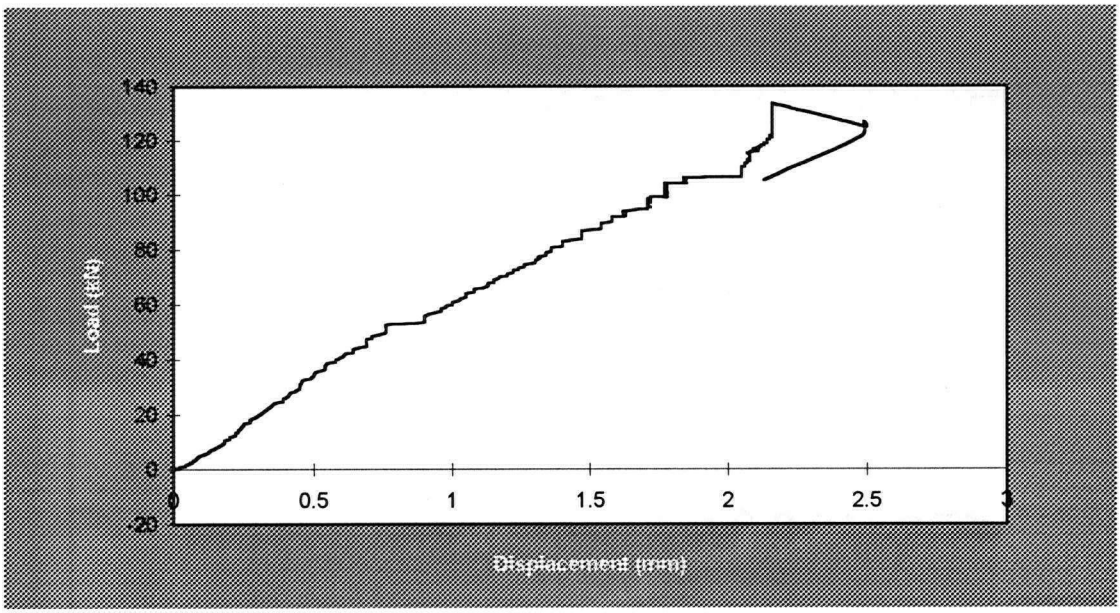


Figure 30. Typical load-deflection curve of full size beam test.

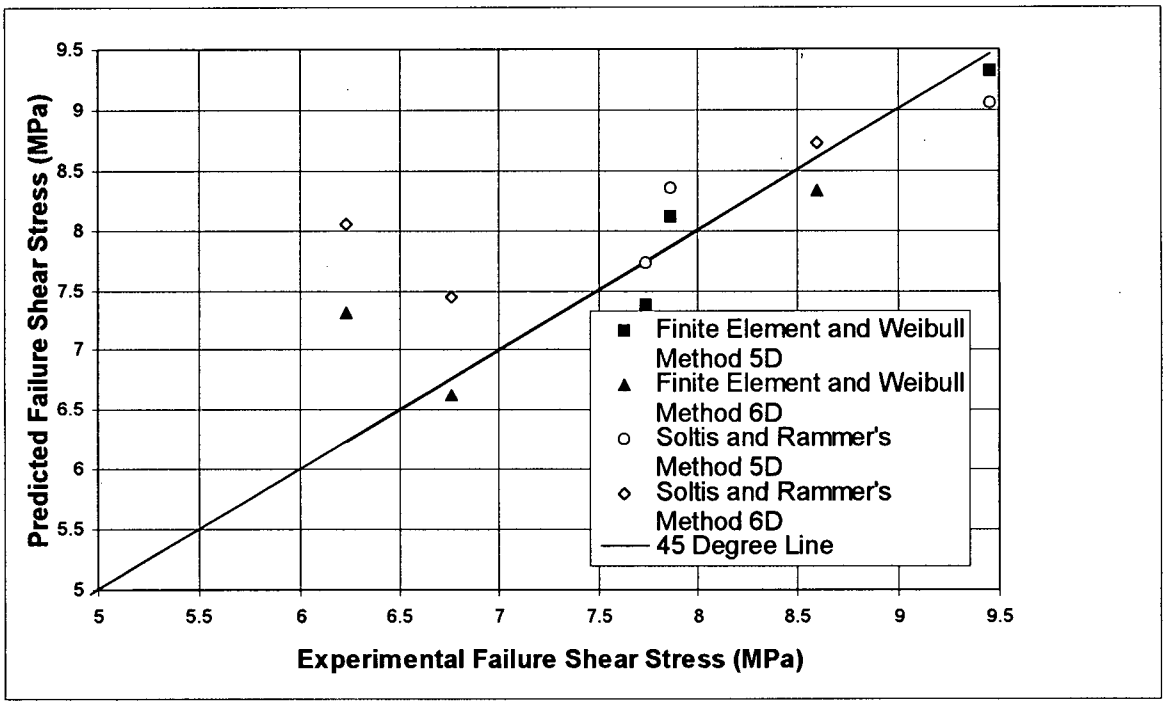


Figure 31. Plot of predicted versus experimental failure stresses ( 38 mm x 185 mm)

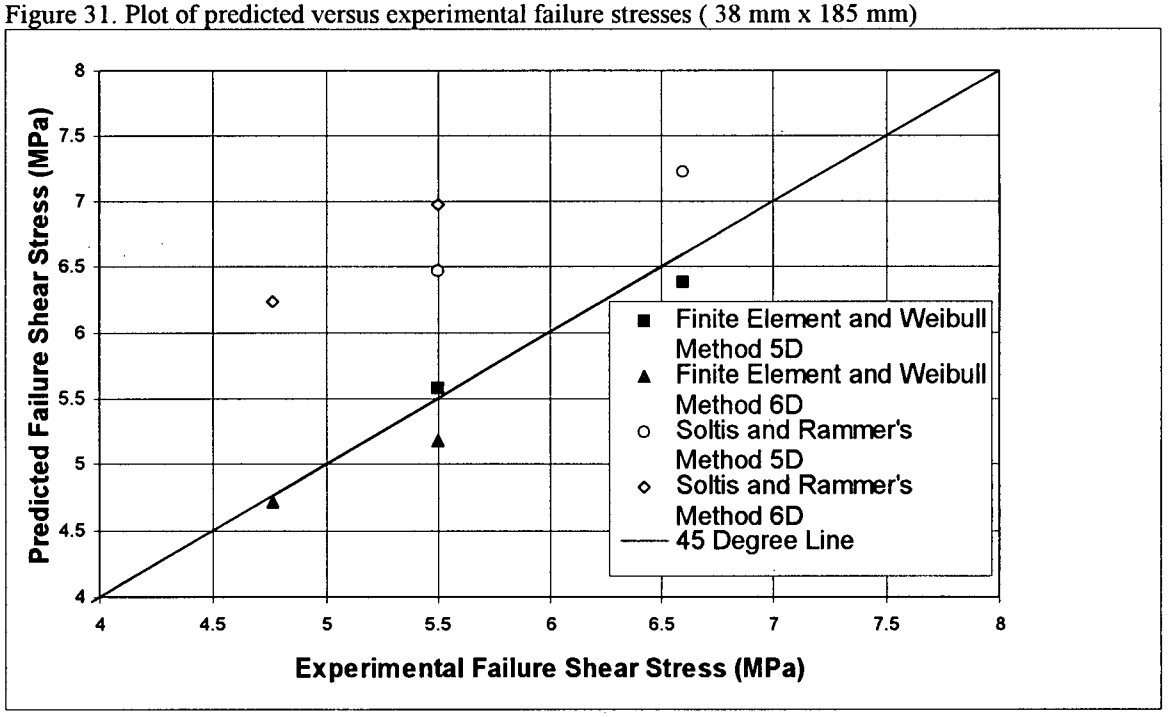


Figure 32. Plot of predicted versus experimental failure stresses ( 38 mm x 285 mm)